https://doi.org/10.5194/egusphere-2025-6329
Preprint. Discussion started: 3 February 2026

Assessing the seasonal compartmentalization of water fluxes in the soil-plant-atmosphere continuum of a high-elevation mountain grassland

Alessio Gentile[1], Davide Gisolo[1], Stefano Brighenti[2,3], Giulia Zuecco[4,5], Chiara Marchina[4], Davide Canone[1], Tanzeel Hamza[1], Stefano Ferrari[1], Stefano Bechis[1] and Stefano Ferraris[1]

[1] Interuniversity Department of Regional and Urban Studies and Planning (DIST), University of Torino and Polytechnic University of Torino, 10125, Torino, Italy
[2] Faculty of Science and Technology, Free University of Bozen-Bolzano, 39100, Bozen-Bolzano, Italy
[3] Eco Research, 39100, Bozen-Bolzano, Italy
[4] Department of Land, Environment, Agriculture and Forestry (TESAF), University of Padova, 35020, Legnaro (PD), Italy
[5] Department of Chemical Sciences (DiSC), University of Padova, 35131, Padova, Italy

Correspondence to: Alessio Gentile (alessio.gentile@unito.it)

Abstract. Improving our understanding of snow–groundwater connectivity remains a key challenge in high-elevation mountain environments. This calls for a multidisciplinary and multimethod research framework that integrates different types of field observations, including the collection of water samples from diverse sources for stable isotope analysis. However, in remote alpine areas, the limited frequency of sampling hinders the generation of robust, data-driven insights into ecohydrological processes. Therefore, accurately modelling water movement and stable isotope transport through soil, vegetation, and groundwater recharge is essential for advancing our understanding of the hydrological functioning of high-altitude ecosystems.

In this work, we combine a recently introduced snow isotope model with the HYDRUS-1D model to simulate water fluxes and isotope transport within the soil–plant–atmosphere continuum of a high-elevation mountain grassland located in the Aosta Valley, north-western Italy. We use this modelling framework to:

I) investigate the seasonal origin of two key water fluxes, namely transpiration and deep drainage (the latter assumed to contribute to groundwater recharge)
II) clarify how seasonal water inputs and root water uptake patterns contribute to ecohydrological separation.

The results reveal the effectiveness of the proposed modelling framework in accurately simulating volumetric water content, actual evapotranspiration, and isotope dynamics at the study site. Based on the model outputs, a higher degree of separation between the water used by plants and the water contributing to deep drainage is observed during intense snowmelt periods. Under these conditions, meltwater (winter water) rapidly drains through the lower soil layers, whereas rainfall (summer water), which predominantly occurs after the snowmelt period, remains in the soil longer, sustaining plant transpiration. However, in 2022, we observed a shift in hydrological functioning: a greater proportion of winter water contributed to

https://doi.org/10.5194/egusphere-2025-6329
Preprint. Discussion started: 3 February 2026

transpiration fluxes under drought conditions. This finding offers valuable insight into how mountain ecosystems may respond to projected increases in temperature and decreases in solid precipitation.

Overall, this work highlights the hydrological conditions that drive the seasonal compartmentalization of water resources in a high-elevation alpine environment, with potential implications for similar mountainous regions worldwide.

1 Introduction

Ecohydrological processes occurring in the subsurface have been often conceptualized relying on physical intuition (Kirchner et al., 2023). However, advancing our understanding of these processes requires detailed insights into the sources and flow paths of subsurface water, which can be gained through emerging measurement techniques (Bovier et al., 2025; Kirchner et al., 2023). In this regard, stable water isotopes (^{18}O, ^{2}H) have been widely used to trace the origin of water taken up by plants, and to distinguish among different geographic-sources that contribute to these fluxes (Ceperley et al., 2024; Orlowski et al., 2023; Sprenger et al., 2016). Although precipitation represents the primary input for plant water uptake, its isotopic composition is highly variable in both space and time. Moreover, only a fraction of precipitation infiltrates the soil and is accessed by roots (Allen et al., 2022); the remainder either runs off at the surface or drains beyond the root zone, contributing to groundwater recharge. As a result, the isotopic signatures ($\delta^{18}O$, $\delta^{2}H$) of plant water and groundwater recharge may diverge from that of the original precipitation (Allen et al., 2022), complicating efforts to trace water sources and flow paths. Despite these challenges, stable isotopes remain a powerful tool in ecohydrological research (White, 1989). They continue to support investigations into questions such as 'From where plants take up water?' (von Freyberg et al., 2020), and "What is the seasonal origin of water used by plants?" (Allen et al., 2019a; Floriancic et al., 2024, 2025).

Previous studies have highlighted the potential for ecohydrological separation between water used by plants and that contributing to groundwater recharge or supplying streamflow (McDonnell, 2014). This concept, known as the *Two Water Worlds* (TWW) hypothesis, proposes that plants access a portion of soil water that is partially disconnected from the water that recharges aquifers and supplies streams (McDonnell, 2017; Evaristo et al., 2015; McDonnell, 2014; Renée Brooks et al., 2010). In essence, this hypothesis posits the existence of two isotopically distinct water pools that exhibit varying degrees of ecohydrological separation bounded by two conceptual extremes (Radolinski et al., 2021; Sprenger and Allen, 2020):

- *Mobile water* moves rapidly through the soil profile and contributes to groundwater recharge and streamflow.
- *Bound water* is retained in the soil matrix and primarily used by plants for transpiration.

These isotopically distinct water pools are visible in the dual-isotope plot due to isotopic fractionation mechanisms (Dubbert et al., 2019; Zhou et al., 2021). Soil and plant water samples frequently plot below the Local Meteoric Water Line (LMWL), whereas groundwater and streamwater typically align with it (Evaristo et al., 2015). These pools could derive from different geographic-sources used by roots that would prefer bound soil water (Dubbert et al., 2019) than mobile water. However, the isotopic composition of extracted water can be affected by the choice of sampling technique and extraction conditions (Allen and Kirchner, 2022; Berry et al., 2018; Chen et al., 2020; Ellsworth and Williams, 2007; Millar et al., 2022; Orlowski et al.,

https://doi.org/10.5194/egusphere-2025-6329
Preprint. Discussion started: 3 February 2026

2016a, b, 2018). Despite these uncertainties, there has been a longstanding call to test the TWW hypothesis across diverse climates and vegetation types (McDonnell, 2014). The ecohydrological community has actively pursued this challenge, but the hypothesis remains one of the most debated and controversial topics in current hydrological research (Dubbert et al., 2019).

For instance, Barbeta and Peñuelas (2017) found that groundwater constitutes a relevant source of water for plants, and that groundwater–plant connectivity may be both more extensive and quantitatively greater than previously reported. Penna et al. (2013), in a study conducted in a small forested catchment in the Italian Pre-Alps, found that beech trees primarily relied on soil water rather than groundwater to support transpiration during late summer and early fall. Radolinski et al. (2021) investigated ecohydrological separation under variable preferential flow conditions using soil columns with varying macropore structures. Their results suggest that mobile water, moving through preferential flow paths, can remain separated from less mobile water and that such separation is most likely to occur following high-intensity precipitation events. Dubbert et al. (2019), based on results obtained by combining $\delta^{18}O$ and $\delta^{2}H$ of precipitation, groundwater, soil and xylem water of *Quercus suber* and *Cistus ladanifer* with observations of soil water contents and sap flow, stated that the differences in the isotopic composition between soil and plant water vs groundwater can be fully explained by spatio-temporal dynamics of soil-related hydrological processes. Finkenbiner et al. (2022) analyzed hundreds of model configurations of soil, climate, and mobile/immobile soil-water domain characteristics. They concluded that traditional soil physics alone may be insufficient to reproduce large ecohydrological separation. However, they also noted that previous findings of separation could be influenced by other unmodeled processes such as root water uptake dynamics and the interacting effects of seasonality.

Regarding seasonality, numerous studies have demonstrated the value of $\delta^{18}O$ and $\delta^{2}H$ isotopes in investigating seasonal water dynamics within the soil-plant-atmosphere continuum. Seasonal variations in the isotopic composition of precipitation follow a sinusoidal cycle, with typical summer and winter values representing the upper and lower bounds of the cycle, respectively. These summer- and winter-derived isotopic inputs, characterized by markedly different $\delta^{18}O$ and $\delta^{2}H$ values, serve as endmembers to identify the seasonal origin of water (Allen et al., 2019b, a). Indeed, Allen et al. (2019a) introduced the Seasonal Origin Index (SOI) to assess the seasonal origins of water in soils and vegetation. The SOI ranges from −1 for water derived entirely from winter precipitation to +1 for water derived entirely from summer precipitation. The SOI = 0 implies that similar fractions of summer and winter precipitation contribute to a considered water flux. The scientific literature presents different results concerning the seasonal origin of water used by plants. Allen et al. (2019a) findings showed negative SOI values in plant water, indicating a substantial contribution from winter precipitation: a pattern also observed by Goldsmith et al. (2022) and Floriancic et al. (2024). Conversely, Zuecco et al. (2026), in the same catchment investigated by Penna et al. (2013), found that trees use predominantly summer water. These differences can be due to varying landscape, climate and plant species characteristics of different study sites (Allen et al., 2019a; Kirchner et al., 2023).

A complementary perspective involves examining the seasonal origin of streamflow. Since evapotranspiration (AET) and discharge (Q) together close the water balance, the seasonal origin of AET must, to some extent, be complementary to that of Q (Allen et al., 2019b). In Swiss catchments, for example, SOI in streamflow (SOI_Q) was found to be ≈ 0, reflecting that

https://doi.org/10.5194/egusphere-2025-6329
Preprint. Discussion started: 3 February 2026

streams are sustained by nearly equal fractions of summer and winter precipitation. Thus, the SOI of AET (SOI_{AET}) fluxes approximates zero, i.e., evapotranspiration is also sustained by nearly equal fractions of summer and winter precipitation (Allen et al., 2019b). Despite this somewhat counterintuitive result, variations in the amount and timing of annual precipitation, as well as differences in geology or soil and plant characteristics, may lead to different seasonal contributions to both Q and AET.

In this paper, we aim to determine whether, in regions with pronounced seasonality of water inputs (e.g., mountain regions), the nature of ecohydrological separation may be influenced by the interaction between the timing and magnitude of snowmelt and rainfall events, as well as by the temporal dynamics of root water uptake. Water inputs such as snowmelt and rainfall differ in intensity and frequency, which directly affect soil hydraulic conductivity and, consequently, soil water dynamics. These variations can influence the spatial and temporal availability of water to plants, potentially shaping the degree of separation between mobile and bound water pools. With the aim of pursuing this objective, multidisciplinary approaches, such as the use of conservative tracers and integrated numerical models, have proven valuable, although data scarcity and the inherent complexity of high-elevation sites remain substantial challenges (Gisolo et al., 2025; van Tiel et al., 2024). Among the available models, HYDRUS-1D (Šimůnek et al., 2018) is a widely used and robust software package for simulating water flow and solute transport in variably saturated soils. It incorporates key physical processes (including infiltration, evapotranspiration, root water uptake, and advection–dispersion) offering a comprehensive representation of water and solute dynamics within the soil-plant-atmosphere continuum. Furthermore, HYDRUS-1D enables the simulation of stable water isotope transport in the vadose zone (Nasta et al., 2023; Stumpp et al., 2012).

We follow an approach that integrates meteorological data with field measurements of stable isotopes in precipitation, soil water, plant water, and spring water of a high-elevation mountain grassland. Starting from these data, we employ a modelling framework that integrates a recently introduced snow isotope model and the modified version of HYDRUS-1D (Stumpp et al., 2012) to simulate isotope transport within the soil-plant-atmosphere continuum of this high-elevation ecosystem. Through isotopic composition modeling, we derive the SOI which enables a robust quantification of the seasonal origin of water fluxes (focusing on transpiration and deep drainage fluxes) across multiple years. The study period encompasses years with contrasting hydrological conditions, ranging from very wet to extremely dry. Through the model output, we gain new insights into the hydrological processes shaping the degree of separation between tightly bound soil water and mobile water draining through the soil profile. The integration of isotope measurements with numerical modeling to investigate alpine grassland ecohydrology remains limited, and, according to our knowledge, no study to date has explicitly tested how seasonal variations in water input, typical of high-elevation environments, interact with root water uptake to assess the degree to which the TWW hypothesis holds. Accordingly, we test the following null dichotomous hypothesis (H_0): “Winter precipitation (i.e., snowmelt) rapidly transits the soil profile recharging groundwater and streams, while summer precipitation (i.e., rainfall) remains available to sustain transpiration fluxes”.

https://doi.org/10.5194/egusphere-2025-6329
Preprint. Discussion started: 3 February 2026

2 Material and Methods

2.1 Study site and datasets

Dora del Nivolet (DOR) is a 16.99-km^2 catchment located in the western Italian Alps (Valsavarenche (AO), Aosta Valley) with elevations ranging from 2390 to 3430 m a.s.l (Figure 2b). The DOR catchment (outlet coordinates: 45°31′16.66″ N; 7°10′47.44″ E) exhibits, under current climatic conditions, a snow-dominated hydroclimatic regime with snow typically accumulating from November and persisting until May, when snowmelt begins (Gentile et al., 2023; Painter et al., 2023). In contrast, the summer period is marked by the onset of rainfall events. Daily winter precipitation was estimated at the study site from snow height measurements from an SR50AT sonic sensor (Campbell Scientific, Inc.), while summer rainfall was reconstructed using data from nearby meteorological stations within the Valsavarenche valley. From summer 2022 onward, summer rainfall was directly measured at the study site using a CS125 present weather sensor (Campbell Scientific, Inc.). Between 2018 and 2022, the alpine grassland within the catchment experienced varying meteorological patterns, reflecting a clear trend (Figure 1).

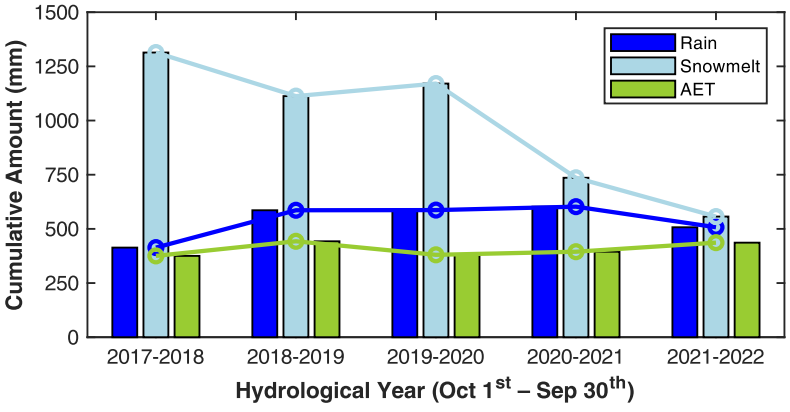

Figure 1 Cumulative values of rainfall, snowmelt, and measured actual evapotranspiration (AET) from hydrological years 2017–2018 to 2021–2022. Each hydrological year spans from October 1st to September 30th of the following year. An exception is made for the year 2017–2018, where measurements begin on November 1st, 2017. Coloured bars represent yearly totals, and lines connect the top of each variable's bars across years to highlight temporal trends. Periods without available AET measurements were filled using linear interpolation prior to annual aggregation. Rainfall and snowmelt values shown in the figure are derived using the model by Ceperley et al. (2020), as described in Section 2.4.

The 2017–2018 hydrological year was exceptionally wet and snowy, followed by two relatively wet years with reduced snowmelt. A notable shift occurred in 2020–2021, when the catchment received decreasing amounts of solid precipitation, resulting in lower snowmelt totals. These conditions intensified in 2021–2022, largely due to a snow drought affecting the Italian Alps during the winter of 2021/22 (Koehler et al., 2022). Over the 2017–2018 to 2021–2022 hydrological years, rainfall remained relatively stable with only minor interannual variability. The same was observed for actual evapotranspiration (AET), which also remained relatively consistent, although it exhibited a slight increase during the 2022 drought. This pattern is consistent with the “drought paradox” described by Mastrotheodoros et al. (2020).

https://doi.org/10.5194/egusphere-2025-6329
Preprint. Discussion started: 3 February 2026

The bedrock geology of the DOR catchment differs between the two sides of the mainstream. The right bank is primarily composed of orthogneisses, granites, metagranites, metagranophyres, porphyroids, and lamprophyric dikes, whereas the left bank features paragneisses, micaschists, and metaconglomerates. Between 2400 and 2600 m a.s.l., talus deposits dominate the right bank, while shallow Dystric Cambisols are prevalent on the left bank (D'Amico et al., 2020b, a). Around 2400 m a.s.l., alpine meadow is characterized by saturated Fluvisols and peat substrates, through which the mainstream flows. The Dystric Cambisols are soils of intermediate development, in which alteration processes have led to the formation of a subsurface cambic horizon (Bw), generally characterized by a brown color and a medium subangular blocky structure. Their formation requires abundant rainfall, or at least a precipitation-to-evapotranspiration ratio favoring the former (D'Amico et al., 2020b, a). The main physical properties of this soil type, reported by D'Amico et al. (2020a), are summarized in Table 1:

Table 1 Main properties of Dystrict Cambisol in the Aosta Valley (D'Amico et al., 2020a)

Horizon type	Organic matter (%)	Sand (%)	Silt (%)	Clay (%)	Texture
A	3.30	63.5	26.9	4.9	Sandy Loam
Bw	0.86	64.6	25.5	4.6	Sandy Loam

The study catchment hosts a diverse range of plant species, including *Gentiana lutea L.*, *Juniperus communis L.*, *Vaccinium myrtillus L.*, *Salix breviserrata Flod.,* and *Trifolium alpinum L.*. For isotopic analysis of plant water, we collected lignified twigs of *Juniperus communis L., Salix breviserrata Flod, Vaccinium myrtillus L.,* along with roots of *Gentiana lutea L.* and *Trifolium alpinum L.,* at monthly intervals from June to October. Despite this botanical diversity, the dominant genus across the catchment is *Festuca* spp. Plant samples were collected on a hillslope located on the left bank of the Dora del Nivolet River, along with soil samples extracted at depths of 10, 20, and 40 cm for isotopic analysis of soil water (Figure 2a). Both plant and soil waters were extracted via cryogenic vacuum distillation (CVD), performed at the Laboratory of the Faculty of Science and Technology, Free University of Bozen-Bolzano (Italy). The CVD system follows the setup described by Koeniger et al. (2011) and further detailed in Zuecco et al. (2022) and Amin et al. (2021). Isotopic analyses were conducted in the same laboratory. Soil water isotopic composition was measured using cavity ring-down spectroscopy (model L2130-i, Picarro Inc., California, USA), while plant water isotopes were analyzed via isotope ratio mass spectrometry (IRMS; Delta V Advantage Conflo IV, Thermo Fisher Scientific Inc., Waltham, MA, USA). The IRMS was coupled with a Thermo Scientific Gas Bench II to determine $\delta^{18}O$ values, following the methodology of Zuecco et al.(2022).

An eddy-covariance station (45°31′8.97″ N; 7°10′17.07″ E) was installed in November 2017 on a small, flat plateau (Figure 2d) with a south–southeast aspect at an elevation of 2555 m a.s.l (Gisolo et al., 2022). The station is equipped with a 3D sonic anemometer (CSAT3B, Campbell Scientific), and a gas analyzer (LI-7500A, Li-Cor). Close to the station (Figure 2d), a precipitation isotope sampler has been installed. In the same location, the soil profile is instrumented at 10, 20, and 40 cm depths with sensors for volumetric water content (10HS, Meter) and matric potential (TEROS 21, Meter). Approximately 400 meters downslope from the eddy-covariance station, on the same hillslope, we monitor a spring (45°31'8.27"N; 7°10'36.21"E)

https://doi.org/10.5194/egusphere-2025-6329
Preprint. Discussion started: 3 February 2026

named "Source" (SOU) (Figure 2c). Spring water levels are recorded at 10-minute intervals using piezoresistive pressure sensors (DL.OCS/N/RS485, STS Sensors), and water samples for isotopic analysis are collected monthly. These samples are analyzed at the Department of Land, Environment, Agriculture and Forestry, University of Padova (Italy), using a liquid water isotope analyzer based on off-axis integrated cavity output spectroscopy (model DLT-100, Los Gatos Research, California, USA).

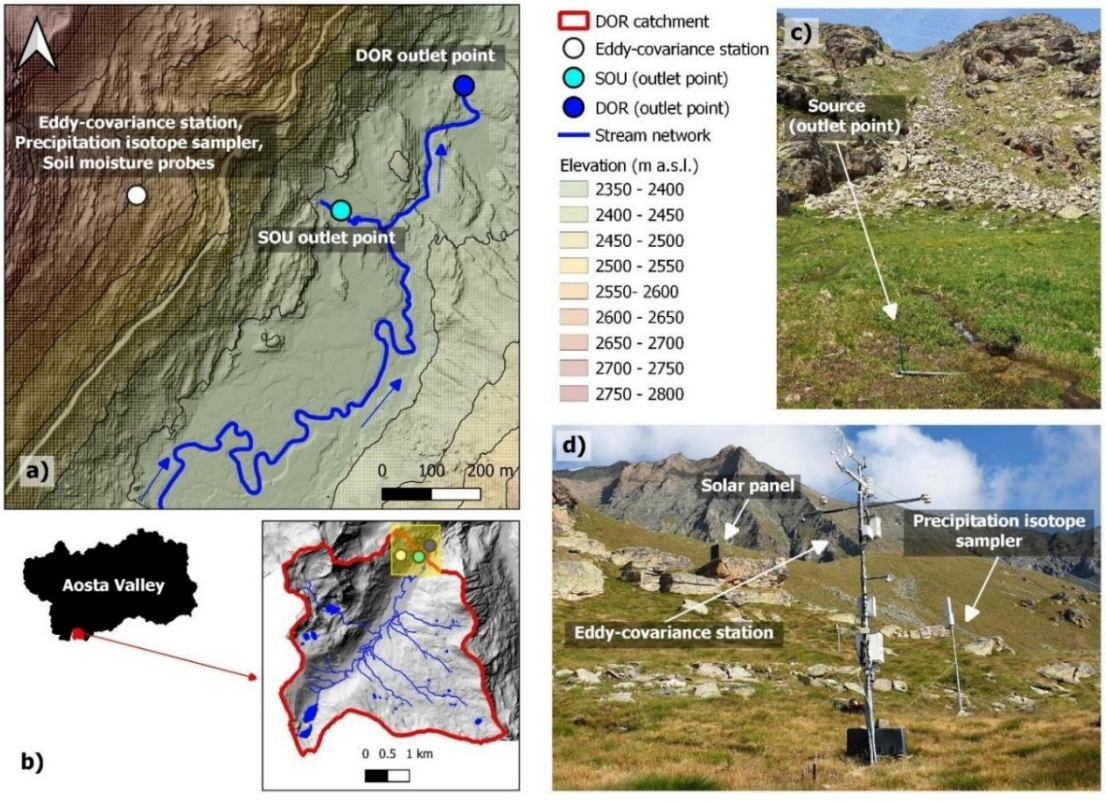

Figure 2 (a) Location of the study site within the Dora del Nivolet (DOR) catchment. Soil samples and lignified twigs/roots are collected nearby the eddy-covariance station where also volumetric water content and matric potential (10, 20, 40 cm depth) are measured. Blue arrows indicate the flow direction (b) Geographical framework of the DOR catchment (c) Photo (02-Jul-2019) of the monitored source (SOU) (d) Photo (23-Aug-2019) of the eddy-covariance station and of the precipitation isotope sampler. In the background it is possible to observe the solar panel that supplies the eddy-covariance station.

2.2 Isotopic fractionation correction

The isotopic composition of the water samples is expressed using the delta notation (δ, in ‰), representing the relative deviation from the Vienna Standard Mean Ocean Water (either V-SMOW or $R_{standard}$):

$$\delta(‰) = \frac{R_{sample} - R_{standard}}{R_{standard}} 1000 \quad (2.1)$$

Where R_{sample} is the isotopic ratio (either $^{18}O/^{16}O$ or $^{2}H/^{1}H$) in the sample, while $R_{standard}$ is the corresponding ratio in the reference standard. Positive δ values indicate enrichment in heavy isotopes relative to the standard, while negative values

https://doi.org/10.5194/egusphere-2025-6329
Preprint. Discussion started: 3 February 2026

indicate depletion. Isotopic fractionation involves changes in the relative abundance of isotopes , such as ^{18}O, ^{16}O, ^{2}H and H, due to differences in the physical behavior of heavy and light isotopes during phase transitions (Scandellari and Penna, 2018). The modified version of HYDRUS-1D (Stumpp et al., 2012) does not account for fractionation processes. Therefore, to ensure comparability between measured and modelled isotopic values, we apply a correction based on the Craig and Gordon (1965) model, which accounts for both equilibrium and kinetic isotopic fractionation during the liquid-to-vapor phase transition. Due to evaporation, the isotopic composition of residual liquid water diverges from the Local Meteoric Water Line (LMWL), forming a so-called evaporation line (Benettin et al., 2018). Using monthly mean air temperature, vapor pressure, and precipitation $\delta^{18}O$ as inputs, we compute the monthly evaporation line slopes. These are then used to reproject the isotopic composition of fractionated soil and plant water samples back to the LMWL. Technical details of the Craig and Gordon (1965) model are provided in Benettin et al. (2018), along with a MATLAB implementation used in this study. To determine whether a water sample is affected by fractionation, we calculate the line-conditioned excess* (lc-excess*) that accounts for uncertainty in the isotopic analysis (Landwehr and Coplen, 2006):

$$\text{lc} - \text{excess}^{*} = \frac{\delta^{2}H - a\delta^{18}O - b}{S_u} \tag{2.2}$$

$$S_u = \sqrt{SD_{\delta^{2}H}^{2} + (a \cdot SD_{\delta^{18}O})^{2}} \tag{2.3}$$

where $\delta^{2}H$ or $\delta^{18}O$ refer to the isotopic composition of the sample, while a and b are the slope and intercept of the LMWL, obtained by linear regression of precipitation isotope data in dual-isotope space (see Section 3.2). $SD_{\delta^{2}H}$ and $SD_{\delta^{18}O}$ denote the standard deviation associated with the isotopic measurement method. For $\delta^{2}H$ and $\delta^{18}O$ measured with the Picarro L2130-i analyzer, SDs are 1.0 ‰ and 0.2 ‰, respectively (Marchina et al., 2020). For measurements conducted using the Isotope Ratio Mass Spectrometer (IRMS) Delta V Advantage (Thermo Fisher Scientific), SDs are 2.5 ‰ and 0.1 ‰, respectively. Samples with negative lc-excess* values are classified as fractionated. For these samples, the intersection points between the LMWL and the corresponding evaporation line are taken to represent their unfractionated isotopic composition. No correction is applied to samples with positive lc-excess* values.

2.3 Estimation of equivalent precipitation (P_{eq}) and its isotopic composition (C_{Peq})

To estimate the timing, quantity, and isotopic composition of liquid water inputs, we employ the snow accumulation, melt, and isotope model developed by Ceperley et al. (2020). While this model involves simplifications compared to more physically detailed snow models, such as *Snowpack* (Lehning et al., 1999), *Crocus* (Brun et al., 1989, 1992; Vionnet et al., 2012), *GEOtop* (Rigon et al., 2006; Endrizzi et al., 2014), *Amundsen* (Strasser et al., 2024) and *FSM* (Essery, 2015), its objective in this study is to simulate the timing and amount of snowmelt so that the snow model could be considered a statistically acceptable proxy for the snow energy balance. In this context, liquid water input refers to rainfall (P_R) and snowmelt (SM) whose combined value is termed equivalent precipitation ($P_{eq} = P_R + SM$). While HYDRUS-1D includes a snow routine similar to that of Ceperley et al. (2020), it does not explicitly simulate the isotopic composition of infiltrating

https://doi.org/10.5194/egusphere-2025-6329
Preprint. Discussion started: 3 February 2026

water from both snowmelt and rainfall, nor their potential mixing (Stumpp et al., 2012). Therefore, the estimation of P_{eq} and its associated isotopic composition (C_{Peq}) is conducted externally to HYDRUS-1D using the Ceperley et al. (2020) model. A brief description of this snow accumulation, melt, and isotope model is provided below. For full technical and methodological details, readers are directed to the original publication, which includes a MATLAB implementation (used in this study) made publicly available by the authors.

2.4 Snow accumulation and melt model

The snow accumulation and melt model proposed by Ceperley et al. (2020) computes snow dynamics at the catchment scale using an elevation band approach. In this study, the DOR catchment is discretized into 100 elevation bands. Snow accumulation and melt are calculated at a daily resolution from November 2017 to February 2023. A key input for these calculations is air temperature (T), which is linearly interpolated across elevation bands using a fixed temperature lapse rate of -3.44 °C per 1000 m. This lapse rate was derived from meteorological data of our monitoring station (see Section 2.1), as well as from additional data provided by the Centro Funzionale Valle d'Aosta, using records from stations located in the Valsavarenche valley: Valsavarenche-Orvieille (2170 m a.s.l.), Valsavarenche-Pont (1951 m a.s.l.) and Valsavarenche Eaux-Rousses (1651 m a.s.l.). Precipitation is held spatially constant across the catchment, as in the original implementation by Ceperley et al. (2020). Since equivalent precipitation (P_{eq}) is computed separately for each elevation band, we used the P_{eq} time series corresponding to the elevation band containing the full experimental setup - eddy-covariance station, soil sensors, and isotope sampling sites (Figure 3a) - as input for HYDRUS-1D.

Within each elevation band, snow accumulation is modeled using a linear temperature-based transition between liquid and solid precipitation (Harpold et al., 2017; Jarvis, 1994). According to Hock (2003), precipitation is classified as snow (P_S) when temperatures are below a lower threshold (T_S), and as rain (P_R) when temperatures exceed an upper threshold (T_R). Snowmelt begins once air temperature surpasses a defined melting threshold (T_0), and is simulated using a degree-day method (Schaefli et al., 2014):

$$SM(t) = \begin{cases} \max[\xi(T(t) - T_0), SWE(t)] & , if\ T(t) > T_0 \\ 0 & , if\ T(t) \leq T_0 \end{cases} \quad (2.4)$$

Where $SM(t)$ is the daily snowmelt (mm d^{-1}) at the time t, $SWE(t)$ is the snow water equivalent (mm) at the time t, and $T(t)$ is the mean daily air temperature (°C) at the time t. ξ (mm $°C^{-1}$ d^{-1}) is the degree-day factor. The parameters used in the model are summarized in Table 2.

Table 2 Parameters used in the snow accumulation and melt model.

Parameter	T_S (°C)	T_R (°C)	T_0 (°C)	ξ (mm $°C^{-1}$ d^{-1})
Value	-2	2	0	4.3

https://doi.org/10.5194/egusphere-2025-6329
Preprint. Discussion started: 3 February 2026

Ideally, these parameters should be calibrated using direct snowmelt observations, which were unavailable in this study. Therefore, we adopted the default values from HYDRUS-1D's internal snow routine, which have shown good consistency with values reported in the literature. For instance, the degree-day factors (ξ) typically range from 1.6 to 6 mm °C^{-1} day^{-1}(Van Mullem et al., 2004), and Ceperley et al. (2020) used ξ values between 2.7 and 5 mm °C^{-1} day^{-1} across three alpine catchments. The HYDRUS-1D default value (ξ = 4.3 mm °C^{-1} day^{-1}) falls within this range and was also used by Stumpp et al. (2012). The temperature thresholds used in snow accumulation models vary across studies. We adopted the T_R and T_S values proposed by Jarvis (1994), consistent with the HYDRUS-1D implementation. The melting threshold T_0 was set to 0 °C, following Schaefli et al. (2014) and Ceperley et al. (2020).

2.5 Snow isotope model

The isotopic composition of water stored in the snowpack (C_S) is computed for each elevation band based on three key assumptions:

1. Complete water mixing within the snowpack.
2. Any rainfall falling on an existing snowpack mixes with the water stored within it.
3. Rainfall mixing with the snowpack is assumed to exit the system within the same time step (t).

The first assumption is generally valid during peak snowmelt periods, when the snowpack is isothermal, but less accurate during early or intermittent melt events (Ceperley et al., 2020). The third assumption simplifies the process by neglecting the snowpack's water holding capacity and the potential for temporary refreezing (Schaefli et al., 2014).

Under these assumptions, the snowpack isotopic mass balance equation can be defined as follows (Ceperley et al., 2020):

$$\frac{d(SWE(t)\cdot C_S(t))}{dt} = C_{P-fit}(t)\cdot P(t) - C_S(t)\cdot P_{eq}(t) \quad (2.5)$$

Where $C_{P\text{-}fit}(t)$ is the isotopic composition of precipitation ($P(t)$) at the time t, derived by fitting a sine curve to observed data, and $C_S(t)$ is the isotopic composition of the water stored in the snowpack at the time t. During time steps in which $SWE(t) + P_{eq}(t) > 0$, the input isotopic composition is $C_S(t)$, which is computed by numerically solving Equation (2.5) through a time-stepping approach, initialized with: $C_S(t_0) = C_{P\text{-}fit}(t_0)$. Else, the input isotopic composition is $C_{P\text{-}fit}$. Since the isotopic composition of equivalent precipitation (C_{Peq}) is computed for each elevation band, we used the C_{Peq} time series corresponding to the elevation band containing the full experimental setup - eddy-covariance station, soil sensors, and isotope sampling sites (Figure 3a) - as input for HYDRUS-1D.

https://doi.org/10.5194/egusphere-2025-6329
Preprint. Discussion started: 3 February 2026

2.6 Potential evapotranspiration (ET_0), evaporation (E_P) and transpiration (T_P)

To compute the potential evapotranspiration (ET_0), we adopt the approach proposed by Ravazzani et al. (2012), who calibrated a modified version of the Hargreaves–Samani (*HS*) equation using evapotranspiration data derived from the FAO-56 Penman–Monteith method. Their modification introduces a correction factor that incorporates two calibration parameters along with the elevation of the meteorological station ($Elev_S$). The calibration was performed for the Upper Po and Rhone River basins, thereby including our study area within the Alpine domain considered by Ravazzani et al. (2012). The resulting modified Hargreaves–Samani equation (*HSM*) is used to compute daily ET_0 as follows:

$$ET_{0,HSM}(t) = (0.817 + 0.00022 \cdot Elev_S) \cdot HC \cdot R_a \cdot (T_{max}(t) - T_{min}(t))^{HE} \cdot \left(\frac{T_{max}(t)+T_{min}(t)}{2} + HT\right) \quad (2.6)$$

Where $ET_{0,HSM}$ (mm d^{-1}) is the daily potential evapotranspiration computed with *HSM* (Figure 3d), $Elev_S$ (m a.s.l.) is the station elevation (2555 m a.s.l. in our study), *HC* is an empirical coefficient equal to 0.0023, R_a (mm d^{-1}) is the extraterrestrial radiation, *HE* is an empirical exponent equal to 0.5, *HT* is a factor used to convert units from Fahrenheit to Celsius and equal to 17.8, T_{max} (°C) is the daily maximum air temperature (Figure 3b) and T_{min} (°C) is the daily minimum air temperature (Figure 3b).

$ET_{0,HSM}$ is then partitioned into potential evaporation (E_P) and potential transpiration (T_P) using the following expressions:

$$E_P(t) = ET_{0,HSM}(t)e^{-k \cdot LAI(t)} \quad (2.7)$$

$$T_P(t) = ET_{0,HSM}(t) - E_P(t) \quad (2.8)$$

Here, k = 0.463 is the extinction coefficient for global solar radiation within the canopy (Ritchie, 1972), and *LAI* is the Leaf Area Index (Figure 3c). The LAI time series (November 2017 to February 2023) was derived using a Google Earth Engine script applied to the MODIS/061/MCD15A3H image collection (spatial resolution: 500 m; temporal resolution: 4 days) for the pixel encompassing the eddy-covariance station. To obtain daily values, linear interpolation was performed between 4-day intervals. The resulting daily time series of E_P and T_P (Figure 3d) are used as input to HYDRUS-1D.

https://doi.org/10.5194/egusphere-2025-6329
Preprint. Discussion started: 3 February 2026

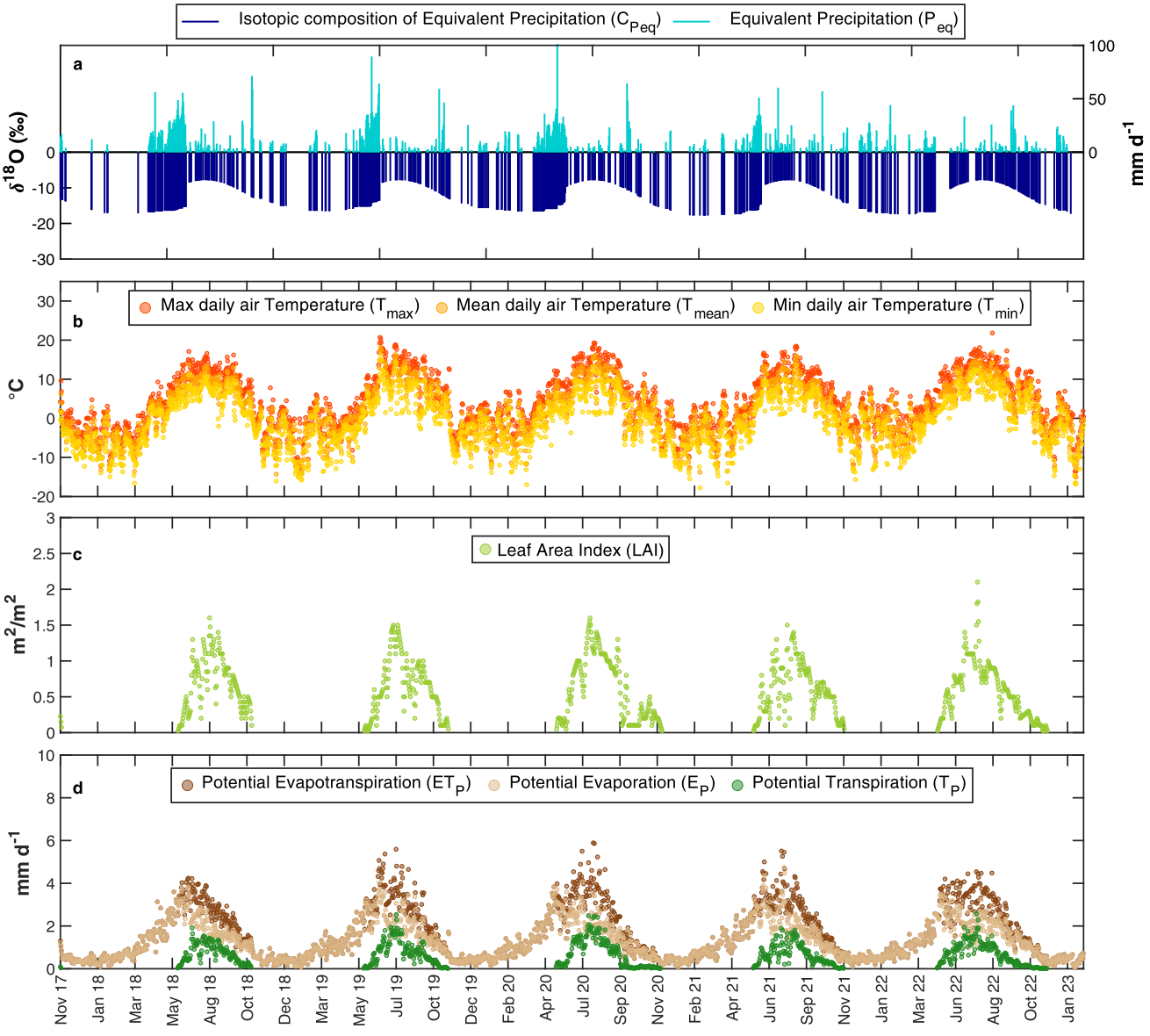

Figure 3 HYDRUS-1D input and related data obtained as described in Sections 2.3-2.6. (a) Equivalent precipitation and corresponding isotopic composition, (b) maximum, mean and minimum daily air temperature, (c) Leaf Area Index, (d) Potential evapotranspiration, evaporation and transpiration. Panels (a) and (d) show data of the time-variable boundary condition inputs used in HYDRUS-1D, while panels (b) and (c) present the intermediate variables used to compute the inputs in panel (d). Prior to importing these inputs into HYDRUS-1D, all fluxes were converted from mm d^{-1} to cm $d^{-1}$and a positive constant was added to the isotopic compositions of equivalent precipitation to ensure all values were positive to run HYDRUS-1D (Stumpp et al., 2012).

https://doi.org/10.5194/egusphere-2025-6329
Preprint. Discussion started: 3 February 2026

2.7 HYDRUS-1D: main equations and model set up

The methodological sections above describe how the input data (Figure 3) were obtained for simulating water flow and isotope transport within the soil profile using HYDRUS-1D (Stumpp et al., 2012). HYDRUS-1D (Šimůnek et al., 2018) simulates variably saturated water flow by solving Richards' equation:

$$\frac{\partial \theta}{\partial t} = -\frac{\partial q}{\partial z} = \frac{\partial}{\partial z}\left[K(h)\frac{\partial h}{\partial z} + K(h)\right] - S \tag{2.9}$$

Where θ is the volumetric water content (cm^3 cm^{-3}), z is the depth below soil surface (positive upward, in cm), q is the water flux (cm d^{-1}), t is time (d), S is a sink term representing root water uptake (d^{-1}), and $K(h)$ is the soil hydraulic conductivity (cm d^{-1}), which is a function of pressure head h (cm) and θ. The soil water retention curve $\theta(h)$ and the hydraulic conductivity function $K(h)$ are described by the van Genuchten (1980) and Mualem (1976) models, respectively:

$$\theta(h) = \begin{cases} \theta_r + \frac{\theta_s - \theta_r}{(1+|\alpha h|^n)^m} & h < 0 \\ \theta_s & h \geq 0 \end{cases} \tag{2.10}$$

$$K(h) = K_s \frac{\left[1-(\alpha h)^{n-1}[1+(\alpha h)^n]^{-m}\right]^2}{[1+(\alpha h)^n]^{\frac{m}{2}}} \tag{2.11}$$

Where θ_r and θ_s (cm^3 cm^{-3}) are the residual and saturated water contents, respectively; α (cm^{-1}), n and m (=1-n^{-1}) are empirical shape parameters; and K_s is the saturated hydraulic conductivity (cm d^{-1}). Root water uptake is simulated using the stress response function of Feddes and Zaradny (1978) with parameters for *grass* selected from the HYDRUS-1D internal database. Root depth was observed to extend down to 60 cm (equal to the modelled soil profile depth), and roots distribution is assumed to be homogeneous throughout the profile (Stumpp et al., 2012). Isotope transport is modeled using the advection–dispersion equation:

$$\frac{\partial(\theta C)}{\partial t} = \frac{\partial}{\partial z}\left(\theta D \frac{\partial C}{\partial z}\right) - \frac{\partial(qC)}{\partial z} - SC \tag{2.12}$$

Where C is the tracer concentration (‰), D (cm^2 d^{-1}) is the dispersion coefficient and S (d^{-1}) is the root water uptake. The dispersion coefficient D is calculated based on Bear (1972) for one-dimensional transport:

$$D = \frac{\lambda_L q}{\theta} + D_w \tau_w \tag{2.13}$$

Where λ_L is the longitudinal dispersivity (cm), D_w is the molecular diffusion coefficient in free water (10^{-9} m^2 s^{-1}) and τ_w is the tortuosity factor of Millington and Quirk (1961).

Two assumptions are made in the isotope transport modeling:

- evaporation does not fractionate water, meaning water and isotopes exit at the same rate at the upper boundary (Stumpp et al., 2012)
- root water uptake does not induce isotopic fractionation.

https://doi.org/10.5194/egusphere-2025-6329
Preprint. Discussion started: 3 February 2026

Model parameters for water flow and isotope transport are calibrated using the inverse modeling tool embedded in HYDRUS-1D, which employs the Marquardt–Levenberg optimization algorithm. Observations used for calibration include volumetric water content, pressure head, and isotopic composition at depths of 10, 20, and 40 cm, whereas model validation relied on observed evapotranspiration and xylem water isotopic composition. A schematic overview of the HYDRUS-1D model setup is provided in Figure 4:

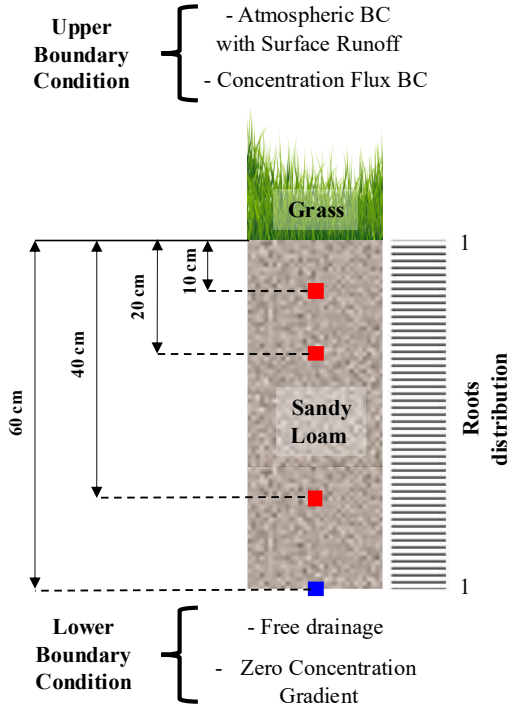

Figure 4 HYDRUS-1D setup. Red squares indicate observation points in which isotope and soil probes measurements are available. Blue square indicates an observation point in which measurements are not available. At the upper boundary, we use the "atmospheric BC with Surface Runoff" condition thus leading both external and soil conditions to control the water flux across the upper boundary. Moreover, we set up a "concentration flux BC", thus specifying liquid phase concentration of the infiltrating water. At the lower boundary, we set up "free drainage (zero gradient)" BC that well describes water flow (solute transport) in the vadose zone field studies.

2.8 The Seasonal Origin Index (SOI)

To assess whether a seasonal separation exists between the water used by plants and the water contributing to groundwater recharge and streamflow, we calculate the Seasonal Origin Index (SOI) following Allen et al.(2019a):

$$SOI = \begin{cases} \frac{\delta_x - \delta_{annP}}{\delta_{summerP} - \delta_{annP}}, \text{if } \delta_x > \delta_{annP} \\ \frac{\delta_x - \delta_{annP}}{\delta_{annP} - \delta_{winterP}}, \text{if } \delta_x < \delta_{annP} \end{cases} \quad (2.14)$$

https://doi.org/10.5194/egusphere-2025-6329
Preprint. Discussion started: 3 February 2026

where δ_x denotes the fractionation-compensated isotopic composition of the considered flux, while $\delta_{winterP}$, $\delta_{summerP}$, and δ_{annP} correspond to the isotopic compositions of typical winter, typical summer, and volume-weighted annual precipitation, respectively. The values of $\delta_{winterP}$ and $\delta_{summerP}$ are defined as the minimum (−18.12 ‰) and maximum (−7.85 ‰) of the sinusoidal fit ($C_{P\text{-}fit}$) describing the seasonal precipitation isotope cycle, whereas δ_{annP} (-13.28 ‰) is derived directly from the observational dataset. The SOI ranges from −1 for water derived entirely from winter precipitation to +1 for water derived entirely from summer precipitation. When considering a given water flux (e.g., transpiration, evaporation, or drainage), SOI = 0 implies that similar fractions of summer and winter precipitation contribute to that flux. In this study, we calculate the SOI by using the isotopic compositions (δ_x) of water fluxes simulated with HYDRUS-1D. We adopt the SOI because, as noted by Allen et al. (2019a), it is specifically designed to assess whether winter or summer precipitation is overrepresented in the considered flux. In other words, the SOI accounts for site-specific seasonality in precipitation, recognizing that, at the study site, we should expect a greater proportion of water fluxes deriving from winter inputs since precipitation is unevenly distributed over the year and predominantly occurs during the winter season. Moreover, this metric has proven to be relatively insensitive to several sources of uncertainty commonly affecting isotope-based rooting depth analyses, particularly those related to sampling and extraction of soil water that accurately represents the water taken up by roots (Allen et al., 2019a; Goldsmith et al., 2019; Orlowski et al., 2018; Penna et al., 2018).

3 Results and Discussion

3.1 Soil hydraulic and solute transport parameters

The optimized soil hydraulic and solute transport parameters are summarized in Table 3:

Table 3 Optimized soil hydraulic and transport parameters

Parameter	K_S (cm d^{-1})	α (cm^{-1})	n (-)	θ_S (cm^3 cm^{-3})	θ_r (cm^3 cm^{-3})	l (-)	λ_L (cm)	ρ (g cm^{-3})
Value	277.93	0.018	1.73	0.54	0.14	0.5	15.44	1.3

The physical plausibility of the optimized parameters is supported by both site-specific measurements and values reported in the literature. The optimized θ_S resulted higher than the maximum volumetric water content (0.43 cm^3 cm^{-3}) measured by soil probes and aligns to the upper limit of typical porosity values for sandy loam soils. Indeed, according to Clapp and Hornberger (1978), a porosity of approximately 0.435± 0.086 is a representative value for this soil texture and defines the upper limit of volumetric water content (Nimmo, 2013). The optimized θ_r is consistent with both the wilting point value at 1500 kPa (0.142 cm^3 cm^{-3}) and the average measured water content for pressure heads exceeding 10^5 cm (0.14 cm^3 cm^{-3}). A non-zero residual water content is further supported by field observations, which showed that even during the extreme drought of 2022, the lowest recorded volumetric water content remained around 0.10 cm³ cm⁻³. By considering the solute travel distance, i.e., the 60 cm soil profile depth, the optimized longitudinal dispersivity λ_L falls within the range of 0.9-20 cm indicated by

https://doi.org/10.5194/egusphere-2025-6329
Preprint. Discussion started: 3 February 2026

Vanderborght and Vereecken (2007) for the 31–80 cm travel distance class. The comparison between measured and optimized soil water retention functions is illustrated in Figure 5:

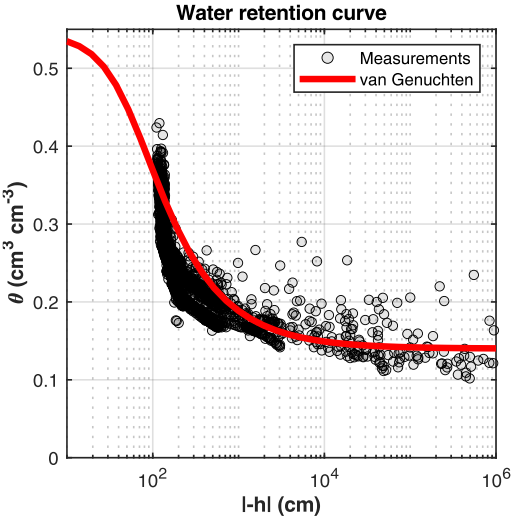

Figure 5 Measured (points) and optimized (lines) water retention function

3.2 Isotopic fractionation correction

Using the Craig and Gordon (1965) model as implemented by Benettin et al. (2018), we derived monthly evaporation slopes (ES) to identify the original isotopic signatures of soil and plant water that had undergone evaporation-driven fractionation. The resulting mean evaporation slope (MES) was 3.39 ± 0.05, with monthly ES values varying modestly from 3.33 in July to 3.49 in May (Figure 6a). The isotopic composition ranges of soil and plant water samples, before and after fractionation correction, are presented in Table 4:

Table 4 Range of isotopic composition of soil and plant water pre- and post- the Craig and Gordon (1965) model application

	Soil water		Plant water	
	Pre-correction	Post-correction	Pre-correction	Post-correction
$\delta^{18}O$ (‰)	-18.2 – -2.9	-18.64 – -5.68	-13.84 – 0.01	-18.96 – -5.65
$\delta^{2}H$ (‰)	-145.88 – -32.92	-145.2 – -32.9	-100.95 – -13.89	-148.66 – -27.24

When compared to the median isotopic composition of precipitation ($\delta^{18}O$: -11.5‰, $\delta^{2}H$: -84.6‰), the median isotopic composition of plant water ($\delta^{18}O$: -10.5‰, $\delta^{2}H$: -70‰) clearly shows enrichment in heavy isotopes, a pattern typical of summer precipitation (Figure 6b). Conversely, the median isotopic composition of spring water at SOU ($\delta^{18}O$: -14.5‰, $\delta^{2}H$: -105.8‰) indicates marked depletion, characteristic of winter precipitation (Figure 6b). The $\delta^{18}O$ and $\delta^{2}H$ values of SOU water are also confined within a narrow range ($\delta^{18}O$: −15.6‰ to −12.8‰; $\delta^{2}H$: −116.6‰ to −95.8‰). These observations provide a first line of evidence for a seasonal partitioning between water sources used by vegetation and those contributing to

https://doi.org/10.5194/egusphere-2025-6329
Preprint. Discussion started: 3 February 2026

streamflow. Specifically, the dual-isotope plot suggests that transpiration fluxes are predominantly supported by summer precipitation, whereas discharge at the SOU spring is mainly sustained by winter precipitation inputs. Interestingly, the median isotopic composition of soil water ($\delta^{18}O$: −11.9‰; $\delta^{2}H$: −84.1‰) closely matches that of precipitation, and both span similar isotopic ranges. In this regard, Radolinski et al. (2021) showed that $\delta^{18}O$ of soil water is more sensitive to changes in precipitation signature than drainage water. A physical explanation of these empirical observations will be provided in Section 3.4, where the HYDRUS-1D results are presented and discussed.

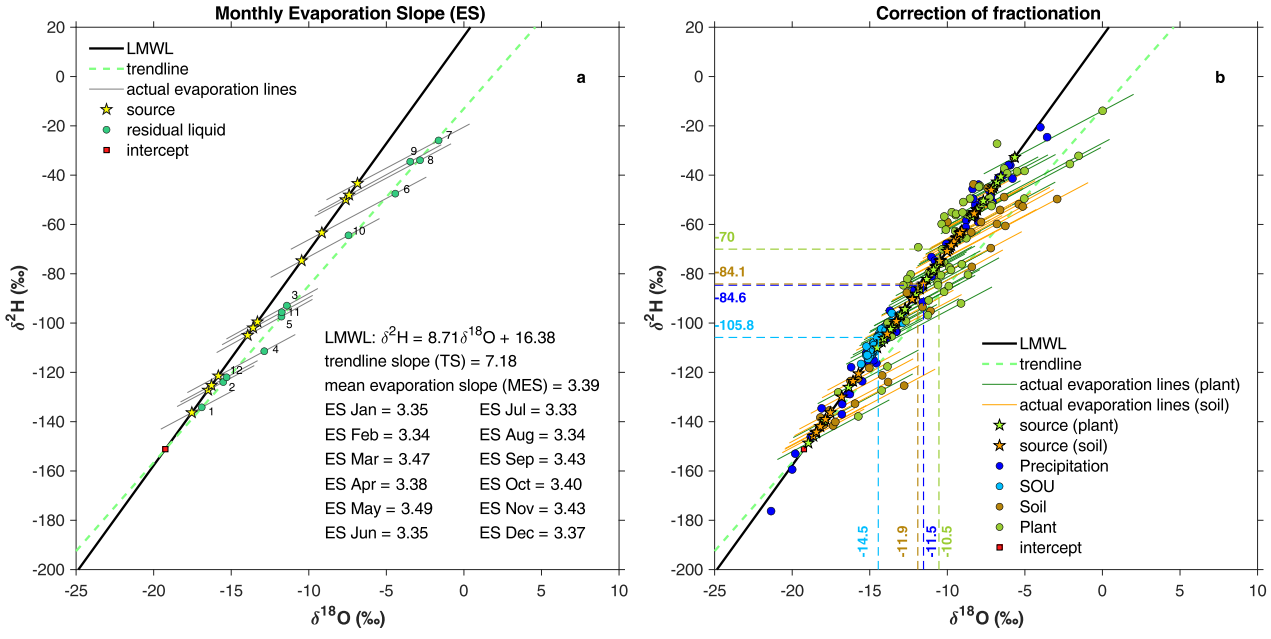

Figure 6 (a) Results of the monthly ES obtained by applying the Craig and Gordon (1965) model being implemented by Benettin et al. (2018). The monthly ES have been used to reproject the fractionated water samples on the LMWL. The numbers next to the residual liquid points indicate the month (1: January; 12: December); (b) Isotopic fractionation correction for fractionated (lc-excess*<0) plant/soil water samples. Precipitation and SOU water samples have been also reported. The median isotopic composition of each reservoir is indicated by the dashed lines.

3.3 Modelled volumetric water content, soil/plant water isotopic composition and actual evapotranspiration

Modelled volumetric water content at the three observation depths (10, 20, and 40 cm) is shown in Figure 7. A strong agreement is observed between modelled and measured values: Spearman's rank correlation coefficient ($\rho_{Pearson}$) = 0.700, 0.720 and 0.723; Mean Absolute Error (MAE) = 0.031, 0.031, 0.028 $cm^3\ cm^{-3}$, Root Mean Square Error (RMSE) = 0.040, 0.039, 0.037 $cm^3\ cm^{-3}$ at 10, 20 and 40 cm, respectively. These results are comparable to performances achieved in other mountainous environments, such as those reported by Bertoldi et al. (2014) using the GEOtop model and Gisolo et al. (2024) using HYDRUS-1D configured for double vegetation. However, some discrepancies between model output and observations are noted, particularly during winter. The peaks in volumetric water content simulated by HYDRUS-1D during winter correspond to modelled snowmelt events. In snow-dominated catchments like DOR, significant winter snowmelt events

https://doi.org/10.5194/egusphere-2025-6329
Preprint. Discussion started: 3 February 2026

contributing to runoff are rare compared to hybrid catchments (Gentile et al., 2023, 2024). Still, minor snowmelt can occur. These events, identified by the degree-day model, coincide with observed declines in snowpack depth (Figure 7d), but they do not translate into measurable increases in volumetric water content. This is likely due to refreezing processes within the snowpack, which are not represented in the model and which inhibit water infiltration during winter (Lundberg et al., 2016; Hirashima et al., 2017; Leroux and Pomeroy, 2017). Accurately capturing the influence of refreezing would require explicitly modelling its effects on both the isotopic composition of snowpack and meltwater over successive melt–freeze cycles: a complexity beyond the scope of this study. Zhou et al. (2008) revealed that the refreezing process would inevitably result in a refrozen snowpack characterized by a line on the dual-isotope plot with a decreased slope compared to solid phase of the initial melting snowpack. Consequently, the line representing the refrozen snowpack on the dual-isotope plot would diminish progressively its slope with each diurnal melt-freeze cycle. On the other side, the line representing the liquid phase on the dual-isotope plot shows an overall slight decrease in the melting period (Zhou et al., 2008).

Further uncertainty arises from estimating the amount and timing of snowmelt at each timestep (Stumpp et al., 2012). Indeed, this is linked to the uncertainty of the parameters used in the degree-day model of Ceperley et al. (2020). The degree-day model relies on air temperature to trigger snowmelt, but in some conditions, it could poorly include the effect of other factors such as topographic shading and proximity to snow-free areas which are identified as further drivers of snowmelt by a stochastic cellular automaton model applied at this site (Painter et al., 2023). In this regard, Bertoldi et al. (2010) highlighted the role of topography, variable precipitation, and solar radiation in shaping volumetric water content patterns, which ultimately affect evapotranspiration. As in our study, also Stumpp et al. (2012), by assessing the effects of land cover and fertilization on water flow and solute transport of five lysimeters using HYDRUS-1D, found the main discrepancies between simulated and measured values because of the uncertainties related to infiltration during snowmelt. Notably, at the end of snowmelt periods, measured volumetric water content is often slightly higher than modelled values. This discrepancy may be explained by the impact of rain-on-snow events, which are typically more intense and short-lived than melt events driven solely by temperature (Myers et al., 2023). Indeed, within the considered elevation range, approximately 26% of the total rainfall between November 2017 and February 2023 occurred under rain-on-snow conditions, that is, precipitation falling as rain while the *SWE* is greater than 0 (Ceperley et al., 2020). Despite these limitations, the degree-day model remains a statistically acceptable proxy for simulating snow energy balance, providing a reasonable approximation of snowmelt timing and magnitude in this high-elevation environment.

https://doi.org/10.5194/egusphere-2025-6329
Preprint. Discussion started: 3 February 2026

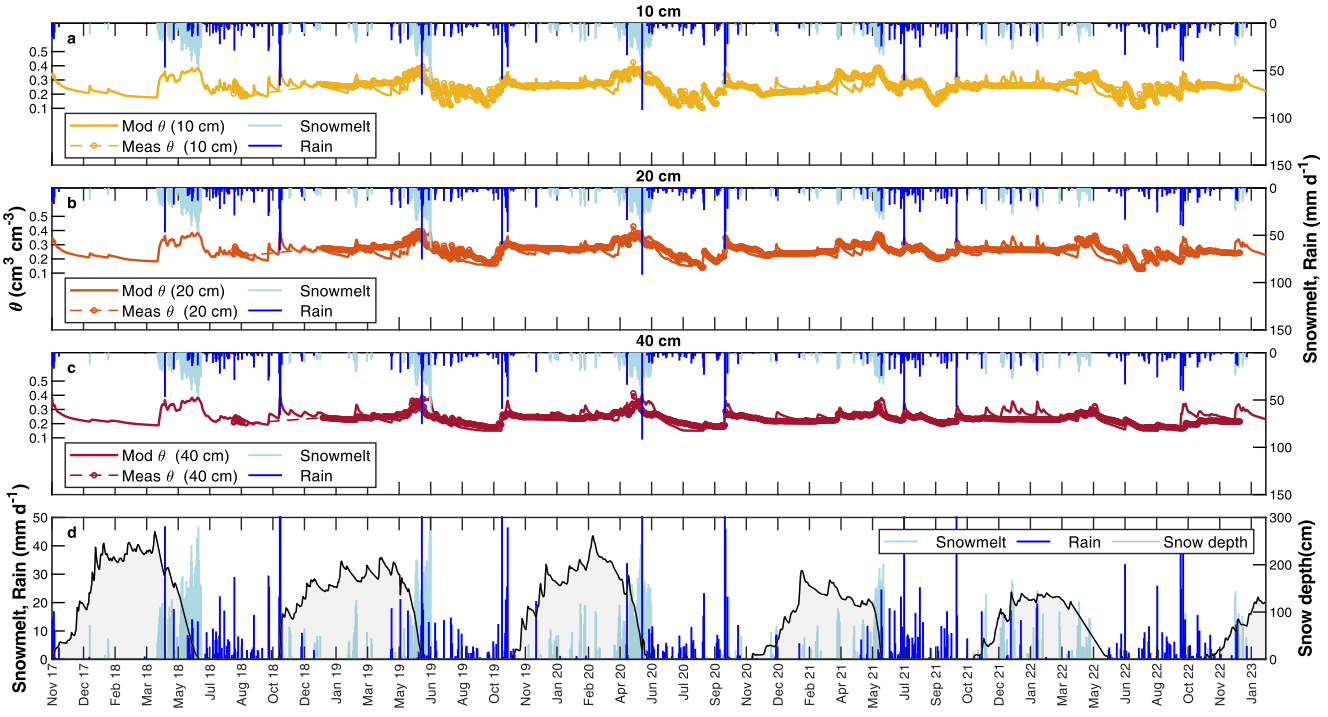

Figure 7 Measured (line with markers) and simulated (line) volumetric water content at (a) 10 cm, (b) 20 cm and (c) 40 cm. Snowmelt and rain have been also indicated. (d) Snow depth, snowmelt and rain.

Modelled isotopic composition of plant water and soil water at the three observation depths (10, 20, and 40 cm) is shown in Figure 8. The estimated $\delta^{18}O$ satisfactorily describe the dynamics of measured soil ($\rho_{Pearson}$= 0.871, 0.359, 0.328; MAE = 1.55, 3.60, 3.70 ‰; RMSE = 1.82, 4.23, 4.09 ‰, at 10,20 and 40 cm, respectively) and plant ($\rho_{Pearson}$= 0.652; MAE = 1.85 ‰; RMSE = 2.35 ‰) water, but with lower accuracy at 20 and 40 cm depths. It is important to consider the uncertainties in isotopic measurements introduced by water extraction techniques. Millar et al. (2022) reviewed the accuracy (expressed as standard deviation, SD) of various extraction methods. For cryogenic vacuum distillation (CVD), the SD of $\delta^{18}O$ can range from 0.09 ‰ to 2.3 ‰. To reflect this methodological uncertainty, the maximum SD values reported by Millar et al. (2022) are displayed as error bars for each measured $\delta^{18}O$ value in Figure 8.

The Ceperley et al. (2020) snow model used in this study includes simplifying assumptions, such as neglecting the snowpack's water holding capacity and temporary refreezing. These assumptions may influence the isotopic composition of equivalent precipitation (C_{Peq}) which in turn affects the modelled $\delta^{18}O$ values of soil and plant water which may therefore show discrepancies compared to the observed $\delta^{18}O$ values. Model performance declines during 2022, particularly at 20 and 40 cm depths. This may be attributed to the assumption of complete mixing within the snowpack, which likely does not hold under conditions of a more ephemeral snowpack, such as those observed in 2022.

https://doi.org/10.5194/egusphere-2025-6329
Preprint. Discussion started: 3 February 2026

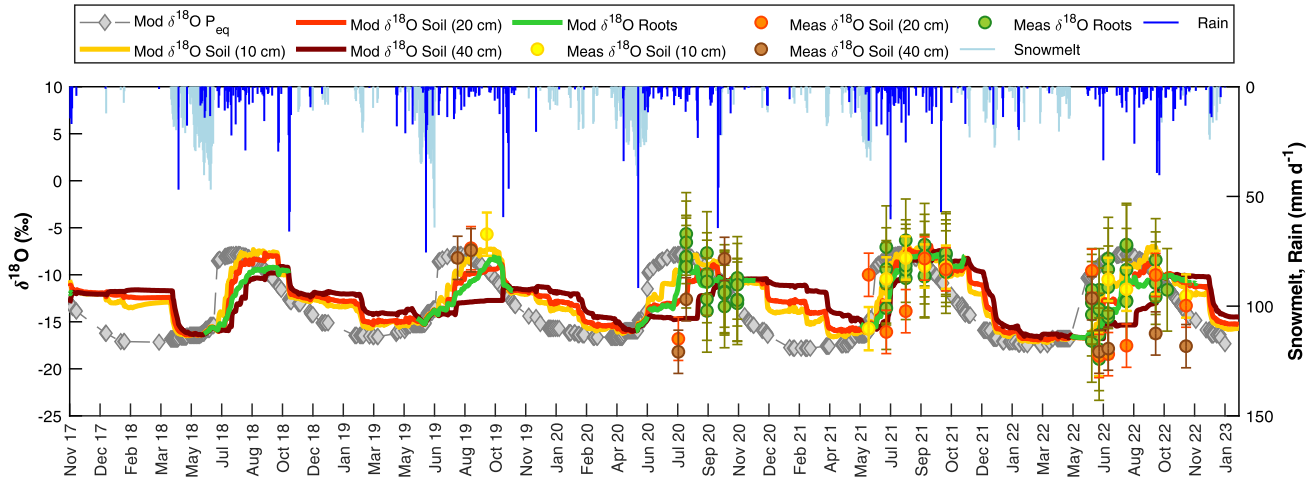

Figure 8 Comparison of modelled soil/plant water isotopic composition at the three observation nodes (10, 20 and 40 cm) and measured soil/plant water isotopic signature. The maximum SD values reported by Millar et al. (2022) are displayed as error bars. Snowmelt, rain and C_{Peq} (when $P_{eq} > 0$) have been also indicated.

The scarcity of wintertime field data in high-elevation environments makes the modelled δ¹⁸O of soil water particularly valuable, as it provides insight into soil hydrological processes that cannot be directly observed during this season. Following the growing season, soil water shows isotopic compositions closer to those of summer precipitation, remaining relatively stable in the absence of early-season snowmelt events that could otherwise modify soil isotopic dynamics during winter. Interestingly, during winter, δ¹⁸O values are less depleted at 40 cm and become progressively more depleted toward the surface. This pattern is reversed during the growing season, with more depleted signatures at deeper soil layers. Such behavior supports the hypothesis that isotopically depleted snowmelt filtrates vertically and contributes to deep drainage during the growing season (Gentile et al., 2023; Cochand et al., 2019; Du et al., 2019; Flerchinger et al., 1992).

To further evaluate the performance of the calibrated HYDRUS-1D parameters for simulating water flow and isotope transport, we compared modelled actual evapotranspiration (AET H-1D) against AET derived from eddy-covariance (AET Eddy) measurements (Figure 9a, Figure 9b). As shown in Figure 9b, a good correspondence was found between modelled and observed AET ($\rho_{Pearson}$ = 0.61, MAE = 0.62 mm d^{-1}, RMSE= 0.88 mm d^{-1}). These performance metrics are consistent with those reported by Gisolo et al. (2024) who simulated evapotranspiration dynamics in an abandoned alpine grassland, also accounting for shrub encroachment, using HYDRUS-1D configured with a double vegetation.

https://doi.org/10.5194/egusphere-2025-6329
Preprint. Discussion started: 3 February 2026

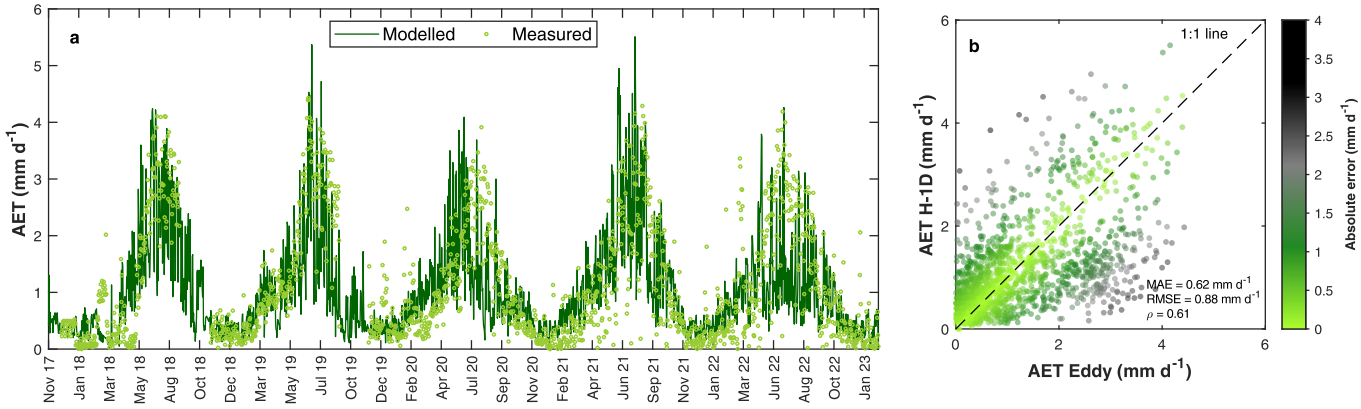

Figure 9 (a) Comparison of AET Eddy and AET H-1D timeseries. (b) AET H-1D versus AET Eddy

3.4 Variable degrees of ecohydrological separation driven by time-variable seasonal water inputs

The comparison between model outputs and observations was used to evaluate the ability of HYDRUS-1D to reproduce volumetric water content, soil and plant water isotopic composition, and actual evapotranspiration in the high-elevation grassland under study. As shown in Section 3.3 the model performs well and produces results consistent with those reported in similar alpine contexts. Building on this validation, we next analyze model outputs to explore the hydrological processes occurring within the soil-plant-atmosphere continuum, with a specific focus on the seasonal partitioning of winter and summer precipitation between plant water uptake and deep drainage (assumed to recharge groundwater). To gain a deeper understanding of this topic, we calculate the SOI (as described in Section 2.8) starting from the modelled isotopic composition of the water fluxes in the soil-plant-atmosphere continuum under study (Figure 10, Figure 11).

Figure 11a presents the simulated equivalent precipitation (P_{eq}) and its SOI. During snowmelt period (mid-April to mid-June), SOI of P_{eq} (SOI_{Peq}) exhibits value close to -1, indicating a dominant contribution from the snow accumulated during winter. In contrast, during late summer (July to September), SOI_{Peq} exhibits value close to 1, indicative of summer rainfall-dominated inputs.

Evaporation is sourced from winter precipitation (i.e., snowmelt) during the snowmelt period and from summer rainfall during the later months (Figure 11b). Indeed, snowmelt recharges the soil predominantly between mid-April to mid-June, while rainfall inputs prevail from July onward.

Transpiration, on the other hand, is largely fed by summer rainfall, as reflected by SOI of transpired water (SOI_T) greater than 0 during the core of the growing season (Figure 11c, Figure 10). This is also evident from the sink term (S), reported in Figure 12e, which peaks from July to August when summer precipitation dominates soil profile inputs, except in 2022 (Figure 12a). These findings are in line with empirical evidence from the Matsch/Mazia catchment in the eastern Alps, where springtime snowmelt does not coincide with peak vegetation activity, leading plants to rely primarily on summer rainfall (Zuecco et al., 2024). Furthermore, our results confirm the finding by Nehemy et al. (2022) that snowmelt can contribute to transpiration early in the growing season, albeit over a brief period, as evidenced from negative SOI_T at the end of May (Figure 11c). This

https://doi.org/10.5194/egusphere-2025-6329
Preprint. Discussion started: 3 February 2026

is also evident in the early increase of the *S* at the end of May (Figure 12e), coinciding with winter-sourced recharge (Figure 12a), though values remain below the *S* peak seen in July–August.

The intense and sustained meltwater inputs lead to the saturation of the soil profile (Figure 12c) and correspond to the highest modeled Darcy velocities (Figure 12d), suggesting enhanced deep filtration of the snowmelt. This is supported by previous findings revealing that snowmelt is generally more effective than rainfall in filtrating beyond the root zone (Earman et al., 2006). Indeed, the SOI of the bottom flux (SOI_{Bot}), representing water that contributes to groundwater recharge, exhibits values clearly below zero between May and June (Figure 11d), indicating a substantial influence of snowmelt during this period. This is consistent with findings from other snow-dominated catchments, where groundwater typically reflects the isotopic composition of snowmelt (Michelon et al., 2023; Pavlovskii et al., 2018). Moreover, past studies revealed that seasonally snow-covered catchments resulted in a snowmelt pulse that enables high groundwater recharge (Ajami et al., 2012; Harrison et al., 2021; Hotovy et al., 2025; Winograd et al., 1998) during summer (Cochand et al., 2019; Du et al., 2019; Flerchinger et al., 1992; Hayashi, 2020). Further support comes from comparing the SOI_{Bot} to that of the monitored spring (Figure 11d, Figure 11e). Despite the bottom flux shows summer signatures ($SOI_{Bot} > 0$) during wintertime (October to February) events (Figure 11d), the SOI of spring water remains slightly lower than 0 (Figure 11e) in this period, suggesting subsurface mixing with winter-sourced storage, likely recharged by snowmelt during the preceding summers.

The previous observations point to a vertical connectivity within the soil profile during snowmelt peaks, where infiltrating water rapidly fills available pore space and microtopographic storage, leading to sudden increases in vertical subsurface flow: a process consistent with the fill-and-spill conceptual model at the plot scale (McDonnell et al., 2021). In this regard, we infer a possible fill-and-spill mechanism at the plot scale (McDonnell et al., 2021). This insight is supported by the timing of peak bottom fluxes, which align with elevated water content and hydraulic conductivity across all soil depths (Figure 12b and Figure 12c), and may be further facilitated by preferential flow pathways in microporous grassland soils (Mohammed et al., 2019).

From Figure 11c,d and Figure 10, in which is reported the SOI_T and SOI_{Bot} during the growing season (1st May-30th Sep), it is possible to observe a high degree of ecohydrological separation of this high-elevation grassland in the years 2018 to 2021. Winter precipitation (e.g., snowmelt) mainly constitutes a mobile water pool that rapidly recharges the groundwater storage (Earman et al., 2006), which in turn supplies streams, so that snowmelt is generally poorly available for plant transpiration. The latter is mainly supplied by a less mobile water pool constituted by summer rainfall that remains available in the soil profile during the core of the growing season. Indeed, the sustained snowmelt pulse was sufficient to saturate the soil, thus explaining the development of vertical connectivity among soil pores. In contrast, summer rainfall events are typically intermittent and, if not intense enough to saturate the soil, they do not generate vertical pore connectivity. This pattern is consistent with Radolinski et al. (2021) asserting that the TWW can occur after intense events.

Interestingly, deviations from this pattern were observed during the 2022 drought (Figure 10). The average SOI_T resulted lower (and negative) than the previous years, thus highlighting a greater snowmelt contribution to these fluxes (Figure 11c). This finding partially aligns with Mastrotheodoros et al. (2020) who observed enhanced evapotranspiration from earlier

https://doi.org/10.5194/egusphere-2025-6329
Preprint. Discussion started: 3 February 2026

snowmelt during the 2003 Alpine drought, thus implying a reduction of groundwater recharge. In our study site, this can be explained by considering an early (i.e., during winter/spring) and more intermittent (i.e., less concentrated and intense) meltwater input with a consequent low hydraulic conductivity *K* and Darcy velocity along the soil profile during the summer of 2022 (Figure 12c, 12d). Most likely, these conditions strongly limit the vertical pore connectivity along the soil profile with a consequent drastic reduction of the bottom flux and with consequent low groundwater storage recharge. Thus, we can observe an enlargement of the time window in which the infiltrated snowmelt is retained in the soil for supplying transpiration along with summer rainfall (Figure 12a). This finding, together with the evidence that snowmelt contributes to transpiration during the early stages of the growing season (Figure 11c), confirms that ecohydrological separation should not be viewed as strict duality, but rather as a matter of "degree of separation" that depends on time-variable and site-specific hydrological dynamics (Kirchner et al., 2023).

Concluding, in light of previous studies suggesting that plants can access soil water disconnected from groundwater and streamflow, we have tested the following null hypothesis (H_0): "Winter precipitation (i.e., snowmelt) rapidly transits the soil profile recharging groundwater and streams, while summer precipitation (i.e., rainfall) remains available to sustain transpiration fluxes" which describes a seasonal nature of the TWW hypothesis. Considering our results, we cannot conclusively accept or reject this hypothesis, as it is framed in a strongly dichotomous manner. In this regard, our findings support the view that it is more appropriate to refer to a degree of ecohydrological separation, which, at our study site, appears more evident in years when snowmelt input is concentrated and continuous, and less pronounced during dry years—when snowmelt input is earlier and intermittent.

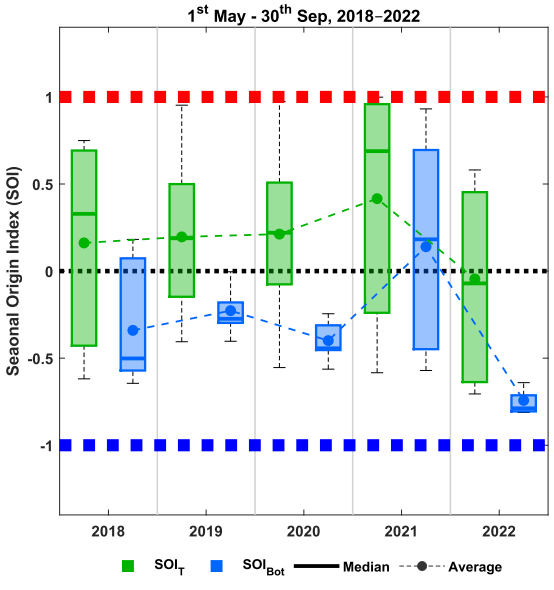

Figure 10 Seasonal Origin Index (SOI) of transpiration and bottom fluxes, simulated with HYDRUS-1D, during the growing seasons from 2018 to 2022.

https://doi.org/10.5194/egusphere-2025-6329
Preprint. Discussion started: 3 February 2026

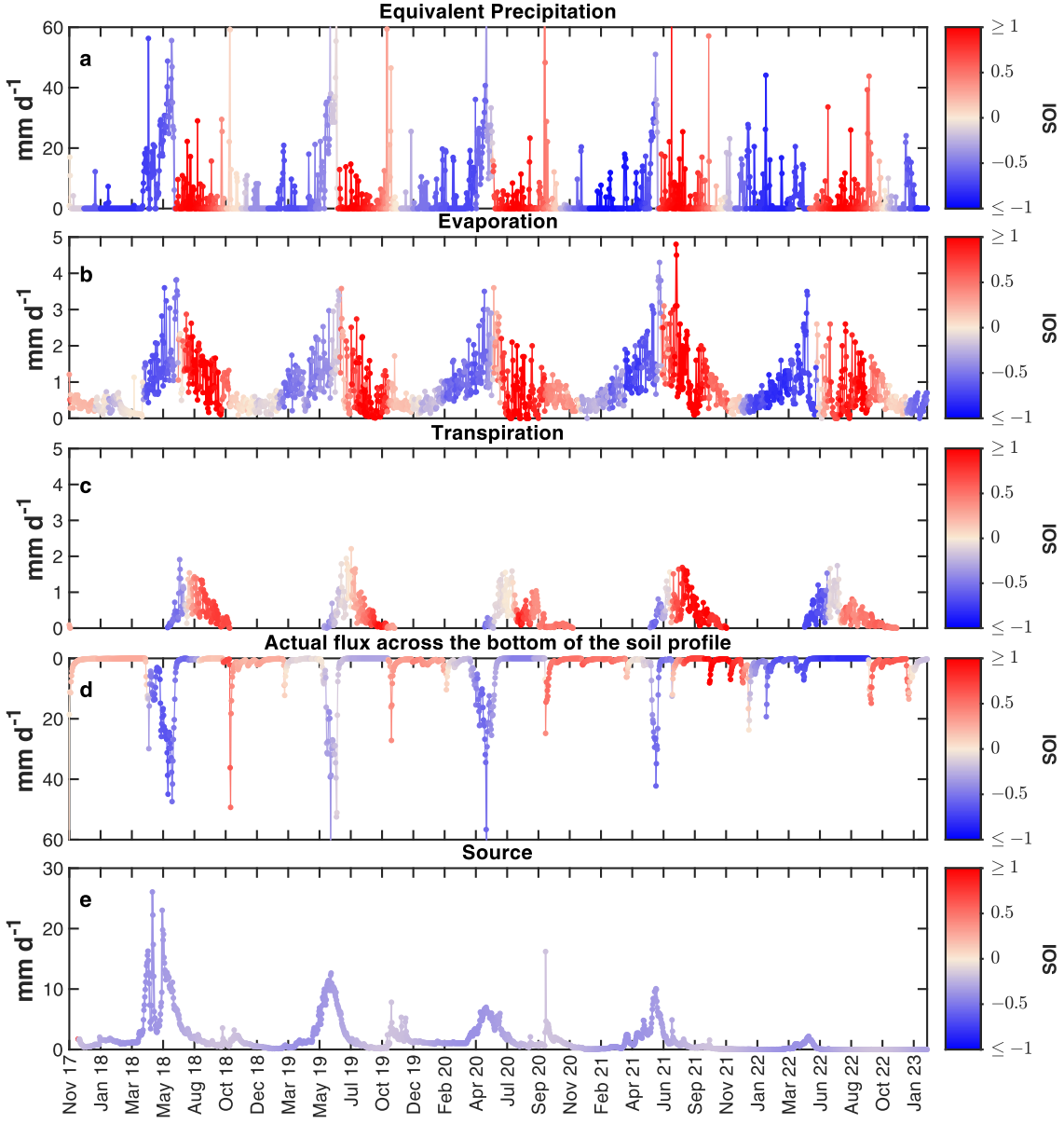

Figure 11 (a) Equivalent precipitation (P_{eq}). (b) Evaporation fluxes. (c) Transpiration fluxes. (d) Actual flux across the bottom of the soil profile. (e) Monitored spring discharge. The red color indicates SOI > 0 (summer water is overrepresented in the flux), while the blue color indicates SOI<0 (winter water is overrepresented in the flux). In panel (a) equivalent precipitation (P_{eq}) and the isotopic composition of equivalent precipitation (C_{Peq}), from which the SOI has been calculated, are obtained with the Ceperley et al. (2020) model. In panels (b), (c) and (d) the fluxes and their isotopic composition, used to retrieve the SOI, are modelled by using HYDRUS-1D. In panel (e) the SOU isotopic composition is derived from measurements: in order to have a continuous isotopic composition (and consequently continuous SOI) at all time-steps we fit a sine function on data as described in von Freyberg et al. (2018).

https://doi.org/10.5194/egusphere-2025-6329
Preprint. Discussion started: 3 February 2026

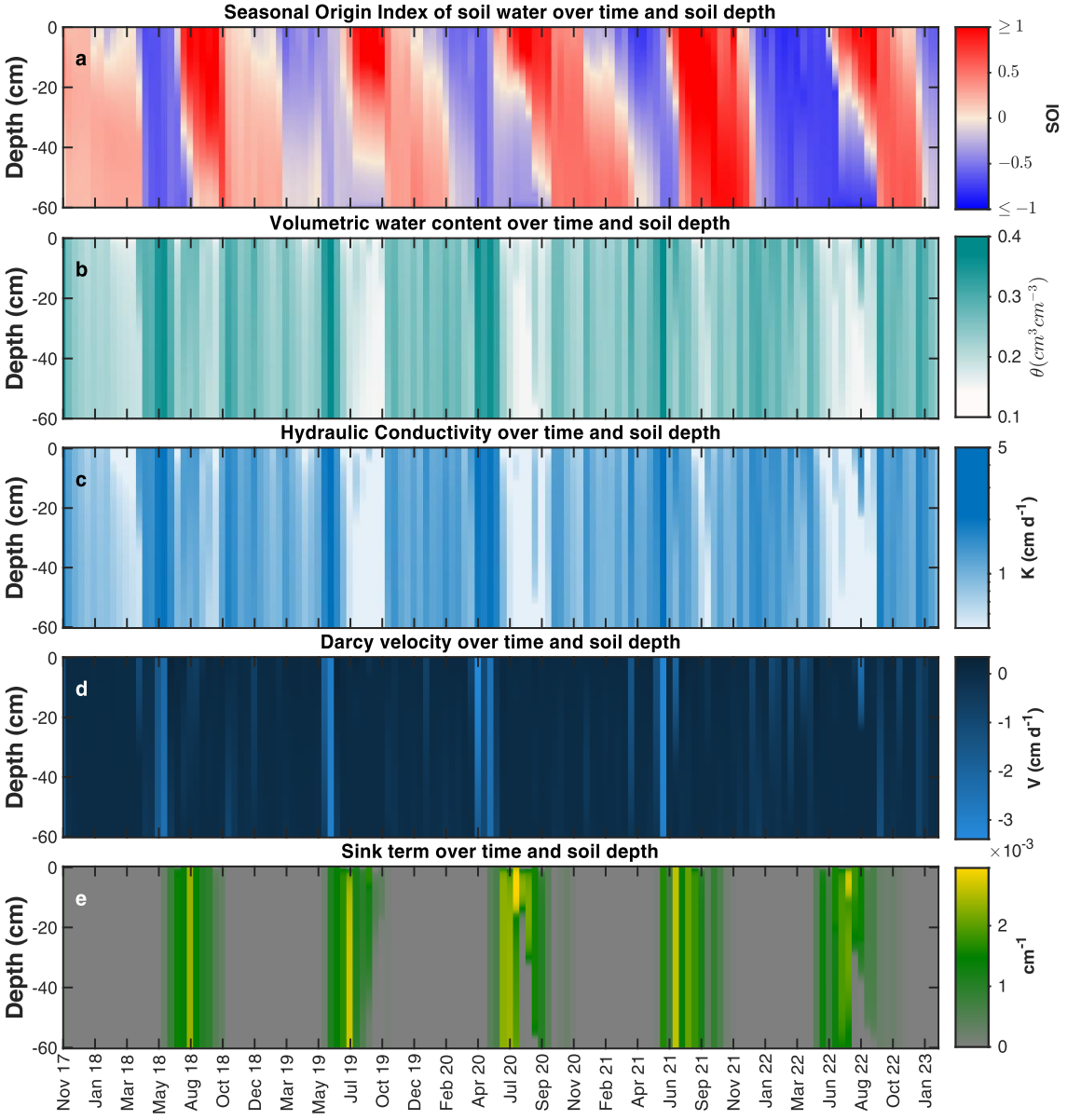

Figure 12 (a) SOI (b) volumetric water content (c) hydraulic conductivity (d) Darcy velocity (the sign convention is positive upwards and negative downwards) and (e) sink term over time and soil depth. Please, note that only 138 print times from 01-Nov-2017 to 06-Feb-2023 with a 14-day time step are reported. In panel (a) the red color indicates SOI > 0 (summer water is overrepresented in the soil water), while the blue color indicates SOI<0 (winter water is overrepresented in the soil water)

https://doi.org/10.5194/egusphere-2025-6329
Preprint. Discussion started: 3 February 2026

4 Conclusions

This study provides new insights into the seasonal partitioning of water resources in a high-elevation alpine grassland, with a particular focus on the degree of ecohydrological separation between seasonal water pools supplying plant transpiration and groundwater recharge. By integrating a snow isotope model with the HYDRUS-1D model, we successfully simulated key water fluxes and their isotopic compositions within the soil–plant–atmosphere continuum under varying hydrometeorological conditions.

Our results demonstrate that, during years with concentrated and sustained snowmelt inputs, a pronounced ecohydrological separation emerges: the snowmelt, due to soil saturation and the possible generation of a vertical pore connectivity, rapidly drains beyond the root zone, contributing to recharge, while summer rainfall is retained in the soil and primarily used by vegetation. However, during the 2022 drought, reduced and more intermittent snowmelt inputs led to lower soil saturation and possibly limited the vertical pore connectivity, enabling winter-sourced snowmelt water to remain accessible to plants for a longer period. This shift resulted in a reduced degree of separation between seasonal water pools, as also indicated by the SOI values of transpiration and bottom fluxes.

These findings suggest that the *Two Water Worlds* (TWW) hypothesis, while useful as a conceptual framework, may oversimplify the dynamic nature of subsurface water partitioning. Rather than a strict duality, our results support the interpretation of ecohydrological separation in this mountain environment as a continuum, with its magnitude modulated by time-variable seasonal water input and root water uptake patterns.

Given projected changes in snow regimes under climate warming, the variability in the degree of ecohydrological separation observed in this study has important implications for anticipating future shifts in ecohydrological functioning within similar mountain ecosystems worldwide.

5 List of Symbols

Symbol	Description
a	Slope of the Local Meteoric Water Line
AET	Actual evapotranspiration (mm d^{-1})
$AET\ H\text{-}1D$	HYDRUS-1D derived actual evapotranspiration (mm d^{-1})
$AET\ Eddy$	AET derived from Eddy-covariance measurements (mm d^{-1})
b	Intercept of the Local Meteoric Water Line
C	Isotopic composition (‰)
C_{Peq}	Isotopic composition of equivalent precipitation (‰) obtained with Ceperley et al. (2020) model
$C_{P\text{-}fit}$	Isotopic composition of precipitation derived by fitting a sine curve to observed data
C_S	Isotopic composition of the snowpack water (‰)obtained with Ceperley et al. (2020) model

https://doi.org/10.5194/egusphere-2025-6329
Preprint. Discussion started: 3 February 2026

CVD	Cryogenic Vacuum Distillation
D	Dispersion coefficient (cm² d⁻¹)
D_w	Molecular diffusion coefficient in free water (m² s⁻¹)
DOR	Dora del Nivolet catchment
$Elev_S$	Monitoring station elevation (m a.s.l.)
E_P	Potential evaporation (mm d⁻¹)
ES	Evaporation slope (-)
ET_0	Potential evapotranspiration (mm d⁻¹)
$ET_{0,HSM}$	Potential evapotranspiration obtained with the Modified Hargreaves–Samani equation (mm d⁻¹)
HC	Empirical coefficient of the Modified Hargreaves–Samani equation
HE	Empirical exponent of the Modified Hargreaves–Samani equation
HS	Hargreaves–Samani equation
HSM	Modified Hargreaves–Samani equation
HT	Factor used to convert units from Fahrenheit to Celsius in the *HSM*
IRMS	Isotope Ratio Mass Spectrometer
k	Extinction coefficient for global solar radiation within the canopy (-)
K	Unsaturated hydraulic conductivity (cm d⁻¹)
Ks	Saturated hydraulic conductivity (cm d⁻¹)
LAI	Leaf Area Index (m² m⁻²)
MAE	Mean Absolute Error
MES	Mean Evaporation Slope (-)
P_R	Rainfall (mm d⁻¹)
P_S	Snowfall (mm d⁻¹)
P_{eq}	Equivalent precipitation (Rainfall + Snowmelt, mm d⁻¹)
R_a	Extraterrestrial radiation (mm d⁻¹)
R_{sample}	Isotopic ratio ($^{18}O/^{16}O$) of the water sample
$R_{standard}$	Isotopic ratio ($^{18}O/^{16}O$) of the reference standard (V-SMOW)
RMSE	Root Mean Square Error
S	Root water uptake sink term (d⁻¹)
S_u	Correction factor for including measurement uncertainty in line-conditioned excess calculation
SD	Standard deviation
$SD_{\delta^{18}O}$	Standard deviation of $\delta^{18}O$ associated with the isotopic analysis method (‰)
$SD_{\delta^{2}H}$	Standard deviation of $\delta^{2}H$ associated with the isotopic analysis method (‰)

https://doi.org/10.5194/egusphere-2025-6329
Preprint. Discussion started: 3 February 2026

SM	Snowmelt (mm d^{-1})
SOI	Seasonal Origin Index (–)
SOI_Q	Seasonal Origin Index of streamflow (–)
SOI_{AET}	Seasonal Origin Index of evapotranspiration (–)
SOI_{Bot}	Seasonal Origin Index of bottom flux (–)
SOI_{Peq}	Seasonal Origin Index of P_{eq} (-)
SOI_T	Seasonal Origin Index of transpiration flux (–)
SOU	"Source": spring within the Dora del Nivolet catchment
SWE	Snow water equivalent (mm)
T	Air temperature (°C)
T_{max}	Daily maximum air temperature (°C)
T_{min}	Daily minimum air temperature (°C)
T_0	*SM* begins once *T* surpasses a defined melting threshold T_0 (°C)
T_R	Precipitation is classified as P_R when *T* exceeds an upper threshold T_R (°C)
T_S	Precipitation is classified as P_S when *T* is below a lower threshold T_S (°C)
TS	Trendline Slope (-)
T_P	Potential transpiration (mm d^{-1})
TWW	Two Water Worlds
h	Pressure head (cm)
*lc-excess**	Line-conditioned excess that accounts for uncertainty in the isotopic analysis
LMWL	Local Meteoric Water Line
m	van Genuchten shape parameter (–), $m = 1 - 1/n$
n	van Genuchten shape parameter (–)
q	Soil water flux (cm d^{-1})
t	Time (days)
z	Depth below soil surface (positive upward, cm)
α	van Genuchten shape parameter (cm^{-1})
δ^2H	Deuterium isotopic composition (‰)
$\delta^{18}O$	Oxygen-18 isotopic composition (‰)
δ_x	Fractionation-compensated isotopic composition of the considered flux (‰)
δ_{annP}	Volume-weighted annual precipitation isotopic composition (‰)
$\delta_{summerP}$	Isotopic composition of typical summer precipitation (‰)
$\delta_{winterP}$	Isotopic composition of typical winter precipitation (‰)

https://doi.org/10.5194/egusphere-2025-6329
Preprint. Discussion started: 3 February 2026

ξ	Degree-day factor (mm °C^{-1} d^{-1})
$\rho_{Pearson}$	Spearman's rank correlation coefficient
θ	Volumetric water content (cm³ cm^{-3})
θ_r	Residual volumetric water content (cm³ cm^{-3})
θ_s	Saturated volumetric water content (cm³ cm^{-3})
λ_L	Longitudinal dispersivity (cm)
τ_w	Tortuosity factor (–)

6 Code and data availability

We use the open-source version 4.17.0140 of HYDRUS-1D freely available from PC-Progress at the following link: https://www.pc-progress.com/en/Default.aspx?H1d-downloads. The computational module of HYDRUS-1D modified for isotopic transport simulation (Stumpp et al., 2012) is freely available from PC-Progress at the following link: https://www.pc-progress.com/en/Default.aspx?h1d-lib-isotope. The MATLAB code for implementing the Craig and Gordon (1965) model for isotopic fractionation correction has been provided by Benettin et al. (2018) and it is freely available from Github at the following link: https://github.com/pbenettin/evaporation-lines. The MATLAB code for calculating the equivalent precipitation with the corresponding isotopic composition has been provided by Ceperley et al. (2020) at https://onlinelibrary.wiley.com/action/downloadSupplement?doi=10.1002%2Fhyp.13937&file=hyp13937-sup-0009-Supinfo2.zip. The Google Earth Engine code for calculating the Leaf Area Index (500 m) from MODIS/061/MCD15A3H image collection is available at the following link: https://code.earthengine.google.com/27d9b4b3960c7e03a72bf4ab1be99923?noload=true (Gentile, 2025).
The data used in this study are available upon reasonable request to the corresponding author.

7 Author contributions

AG identified the research gap and defined the methodology with SFS. AG processed the data to be used as input in HYDRUS-1D with the support of SF, performed the HYDRUS-1D simulations and the post-processing operations. DG, DC and SBE collected soil/plant/water samples at the study site and managed the maintenance activities of the scientific instruments responsible for data production. SBR, GZ and CM performed the isotopic analyses of the collected samples (soil, plant and water). DG managed and processed data from the Eddy-Covariance station with the support of TH. SFS contributed to the acquisition of funding for the projects leading to this publication and supervised the research activity planning and execution. All authors revised the paper and gave final approval to the submitted version.

https://doi.org/10.5194/egusphere-2025-6329
Preprint. Discussion started: 3 February 2026

8 Acknowledgments

This work was supported by the PRIN MIUR 2017SL7ABC_005 WATZON Project, by the PRIN 2022 202295PFKP SUNSET Project and by Funding 2021 Fondazione CRT. The support of the Valsavarenche Municipality and the Gran Paradiso National Park is also gratefully acknowledged. The authors acknowledge the use of ChatGPT for improving the language of the manuscript.

9 Financial support

This publication is part of the project NODES which has received funding from the MUR – M4C2 1.5 of PNRR funded by the European Union - NextGenerationEU (Grant agreement no. ECS00000036).

10 References

Ajami, H., Meixner, T., Dominguez, F., Hogan, J., and Maddock III, T.: Seasonalizing Mountain System Recharge in Semi-Arid Basins-Climate Change Impacts, Groundwater, 50, 585–597, https://doi.org/10.1111/j.1745-6584.2011.00881.x, 2012.

Allen, S. T. and Kirchner, J. W.: Potential effects of cryogenic extraction biases on plant water source partitioning inferred from xylem-water isotope ratios, Hydrol. Process., 36, e14483, https://doi.org/10.1002/hyp.14483, 2022.

Allen, S. T., Kirchner, J. W., Braun, S., Siegwolf, R. T. W., and Goldsmith, G. R.: Seasonal origins of soil water used by trees, Hydrol. Earth Syst. Sci., 23, 1199–1210, https://doi.org/10.5194/hess-23-1199-2019, 2019a.

Allen, S. T., Freyberg, J. von, Weiler, M., Goldsmith, G. R., and Kirchner, J. W.: The Seasonal Origins of Streamwater in Switzerland, Geophys. Res. Lett., 46, 10425–10434, https://doi.org/10.1029/2019GL084552, 2019b.

Allen, S. T., Sprenger, M., Bowen, G. J., and Brooks, J. R.: Spatial and Temporal Variations in Plant Source Water: O and H Isotope Ratios from Precipitation to Xylem Water, in: Stable Isotopes in Tree Rings: Inferring Physiological, Climatic and Environmental Responses, edited by: Siegwolf, R. T. W., Brooks, J. R., Roden, J., and Saurer, M., Springer International Publishing, Cham, 501–535, https://doi.org/10.1007/978-3-030-92698-4_18, 2022.

Amin, A., Zuecco ,Giulia, Marchina ,Chiara, Engel ,Michael, Penna ,Daniele, McDonnell ,Jeffrey J., and and Borga, M.: No evidence of isotopic fractionation in olive trees (Olea europaea): a stable isotope tracing experiment, Hydrol. Sci. J., 66, 2415–2430, https://doi.org/10.1080/02626667.2021.1987440, 2021.

Barbeta, A. and Peñuelas, J.: Relative contribution of groundwater to plant transpiration estimated with stable isotopes, Sci. Rep., 7, 10580, https://doi.org/10.1038/s41598-017-09643-x, 2017.

Bear, J.: Dynamics of Fluids in Porous Media, American Elsevier Pub. Co., 1972.

Benettin, P., Volkmann, T. H. M., von Freyberg, J., Frentress, J., Penna, D., Dawson, T. E., and Kirchner, J. W.: Effects of climatic seasonality on the isotopic composition of evaporating soil waters, Hydrol. Earth Syst. Sci., 22, 2881–2890, https://doi.org/10.5194/hess-22-2881-2018, 2018.

Berry, Z. C., Evaristo, J., Moore, G., Poca, M., Steppe, K., Verrot, L., Asbjornsen, H., Borma, L. S., Bretfeld, M., Hervé-Fernández, P., Seyfried, M., Schwendenmann, L., Sinacore, K., De Wispelaere, L., and McDonnell, J.: The two water worlds

https://doi.org/10.5194/egusphere-2025-6329
Preprint. Discussion started: 3 February 2026

hypothesis: Addressing multiple working hypotheses and proposing a way forward, Ecohydrology, 11, e1843, https://doi.org/10.1002/eco.1843, 2018.

Bertoldi, G., Notarnicola, C., Leitinger, G., Endrizzi, S., Zebisch, M., Della Chiesa, S., and Tappeiner, U.: Topographical and ecohydrological controls on land surface temperature in an alpine catchment, Ecohydrology, 3, 189–204, https://doi.org/10.1002/eco.129, 2010.

Bertoldi, G., Della Chiesa, S., Notarnicola, C., Pasolli, L., Niedrist, G., and Tappeiner, U.: Estimation of soil moisture patterns in mountain grasslands by means of SAR RADARSAT2 images and hydrological modeling, J. Hydrol., 516, 245–257, https://doi.org/10.1016/j.jhydrol.2014.02.018, 2014.

Bovier, M. C., Fedotov, S., Ferraris, S., Gentile, A., and Toaldo, B.: Stochastic model for subsurface water flow in Swiss catchments, Adv. Water Resour., 196, 104883, https://doi.org/10.1016/j.advwatres.2024.104883, 2025.

Brun, E., Martin, E., Simon, V., Gendre, C., and Coleou, C.: An Energy and Mass Model of Snow Cover Suitable for Operational Avalanche Forecasting, J. Glaciol., 35, 333–342, https://doi.org/10.3189/S0022143000009254, 1989.

Brun, E., David, P., Sudul, M., and Brunot, G.: A numerical model to simulate snow-cover stratigraphy for operational avalanche forecasting, J. Glaciol., 38, 13–22, https://doi.org/10.3189/S0022143000009552, 1992.

Ceperley, N., Zuecco, G., Beria, H., Carturan, L., Michelon, A., Penna, D., Larsen, J., and Schaefli, B.: Seasonal snow cover decreases young water fractions in high Alpine catchments, Hydrol. Process., 34, 4794–4813, https://doi.org/10.1002/hyp.13937, 2020.

Ceperley, N., Gimeno, T. E., Jacobs, S. R., Beyer, M., Dubbert, M., Fischer, B., Geris, J., Holko, L., Kübert, A., Le Gall, S., Lehmann, M. M., Llorens, P., Millar, C., Penna, D., Prieto, I., Radolinski, J., Scandellari, F., Stockinger, M., Stumpp, C., Tetzlaff, D., van Meerveld, I., Werner, C., Yildiz, O., Zuecco, G., Barbeta, A., Orlowski, N., and Rothfuss, Y.: Toward a common methodological framework for the sampling, extraction, and isotopic analysis of water in the Critical Zone to study vegetation water use, WIREs Water, 11, e1727, https://doi.org/10.1002/wat2.1727, 2024.

Chen, Y., Helliker, B. R., Tang, X., Li, F., Zhou, Y., and Song, X.: Stem water cryogenic extraction biases estimation in deuterium isotope composition of plant source water, Proc. Natl. Acad. Sci. U. S. A., 117, 33345–33350, https://doi.org/10.1073/pnas.2014422117, 2020.

Clapp, R. B. and Hornberger, G. M.: Empirical equations for some soil hydraulic properties, Water Resour. Res., 14, 601–604, https://doi.org/10.1029/WR014i004p00601, 1978.

Cochand, M., Christe, P., Ornstein, P., and Hunkeler, D.: Groundwater Storage in High Alpine Catchments and Its Contribution to Streamflow, Water Resour. Res., 55, 2613–2630, https://doi.org/10.1029/2018WR022989, 2019.

Craig, H. and Gordon, L. I.: Deuterium and oxygen 18 variations in the ocean and marine atmosphere, 1965.

D'Amico, M. E., Pintaldi, E., Sapino, E., Quaglino, E., Passarella, I., Freppaz, M., Navillod, E., Rocco, R., and Casola, S.: Carta dei Suoli della Valle d'Aosta : Note Illustrative, 2020a.

D'Amico, M. E., Pintaldi, E., Sapino, E., Colombo, N., Quaglino, E., Stanchi, S., Navillod, E., Rocco, R., and Freppaz, M.: Soil types of Aosta Valley (NW-Italy), J. Maps, 16, 755–765, https://doi.org/10.1080/17445647.2020.1821803, 2020b.

https://doi.org/10.5194/egusphere-2025-6329
Preprint. Discussion started: 3 February 2026

Du, X., Fang, M., Lv, H., Cheng, T., Hong, P., and Liu, C.: Effect of snowmelt infiltration on groundwater recharge in a seasonal soil frost area: a case study in Northeast China, Environ. Monit. Assess., 191, 151, https://doi.org/10.1007/s10661-019-7285-7, 2019.

Dubbert, M., Caldeira, M. C., Dubbert, D., and Werner, C.: A pool-weighted perspective on the two-water-worlds hypothesis, New Phytol., 222, 1271–1283, https://doi.org/10.1111/nph.15670, 2019.

Earman, S., Campbell, A. R., Phillips, F. M., and Newman, B. D.: Isotopic exchange between snow and atmospheric water vapor: Estimation of the snowmelt component of groundwater recharge in the southwestern United States, J. Geophys. Res. Atmospheres, 111, https://doi.org/10.1029/2005JD006470, 2006.

Ellsworth, P. Z. and Williams, D. G.: Hydrogen isotope fractionation during water uptake by woody xerophytes, Plant Soil, 291, 93–107, https://doi.org/10.1007/s11104-006-9177-1, 2007.

Endrizzi, S., Gruber, S., Dall'Amico, M., and Rigon, R.: GEOtop 2.0: simulating the combined energy and water balance at and below the land surface accounting for soil freezing, snow cover and terrain effects, Geosci. Model Dev., 7, 2831–2857, https://doi.org/10.5194/gmd-7-2831-2014, 2014.

Essery, R.: A factorial snowpack model (FSM 1.0), Geosci. Model Dev., 8, 3867–3876, https://doi.org/10.5194/gmd-8-3867-2015, 2015.

Evaristo, J., Jasechko, S., and McDonnell, J. J.: Global separation of plant transpiration from groundwater and streamflow, Nature, 525, 91–94, https://doi.org/10.1038/nature14983, 2015.

Feddes, R. A. and Zaradny, H.: Model for simulating soil-water content considering evapotranspiration — Comments, J. Hydrol., 37, 393–397, https://doi.org/10.1016/0022-1694(78)90030-6, 1978.

Finkenbiner, C. E., Good, S. P., Renée Brooks, J., Allen, S. T., and Sasidharan, S.: The extent to which soil hydraulics can explain ecohydrological separation, Nat. Commun., 13, 6492, https://doi.org/10.1038/s41467-022-34215-7, 2022.

Flerchinger, G. N., Cooley, K. R., and Ralston, D. R.: Groundwater response to snowmelt in a mountainous watershed, J. Hydrol., 133, 293–311, https://doi.org/10.1016/0022-1694(92)90260-3, 1992.

Floriancic, M. G., Allen, S. T., and Kirchner, J. W.: Isotopic evidence for seasonal water sources in tree xylem and forest soils, Ecohydrology, n/a, e2641, https://doi.org/10.1002/eco.2641, 2024.

Floriancic, M. G., Goldsmith, G. R., Beria, H., Allen, S. T., and Kirchner, J. W.: Limited Soil Water Recharge in Summer Affects Seasonal Isotopic Signatures of Tree Xylem Water, Ecohydrology, 18, e70077, https://doi.org/10.1002/eco.70077, 2025.

von Freyberg, J., Allen, S. T., Seeger, S., Weiler, M., and Kirchner, J. W.: Sensitivity of young water fractions to hydro-climatic forcing and landscape properties across 22 Swiss catchments, Hydrol. Earth Syst. Sci., 22, 3841–3861, https://doi.org/10.5194/hess-22-3841-2018, 2018.

von Freyberg, J., Allen, S. T., Grossiord, C., and Dawson, T. E.: Plant and root-zone water isotopes are difficult to measure, explain, and predict: Some practical recommendations for determining plant water sources, Methods Ecol. Evol., 11, 1352–1367, https://doi.org/10.1111/2041-210X.13461, 2020.

https://doi.org/10.5194/egusphere-2025-6329
Preprint. Discussion started: 3 February 2026

Gentile, A., Canone, D., Ceperley, N., Gisolo, D., Previati, M., Zuecco, G., Schaefli, B., and Ferraris, S.: Towards a conceptualization of the hydrological processes behind changes of young water fraction with elevation: a focus on mountainous alpine catchments, Hydrol. Earth Syst. Sci., 27, 2301–2323, https://doi.org/10.5194/hess-27-2301-2023, 2023.

Gentile, A., von Freyberg, J., Gisolo, D., Canone, D., and Ferraris, S.: Technical note: Two-component electrical-conductivity-based hydrograph separation employing an exponential mixing model (EXPECT) provides reliable high-temporal-resolution young water fraction estimates in three small Swiss catchments, Hydrol. Earth Syst. Sci., 28, 1915–1934, https://doi.org/10.5194/hess-28-1915-2024, 2024.

van Genuchten, M. Th.: A Closed-form Equation for Predicting the Hydraulic Conductivity of Unsaturated Soils, Soil Sci. Soc. Am. J., 44, 892–898, https://doi.org/10.2136/sssaj1980.03615995004400050002x, 1980.

Gisolo, D., Previati, M., Bevilacqua, I., Canone, D., Boetti, M., Dematteis, N., Balocco, J., Ferrari, S., Gentile, A., Nsassila, M., Heery, B., Vereecken, H., and Ferraris, S.: A Calibration Free Radiation Driven Model for Estimating Actual Evapotranspiration of Mountain Grasslands (CLIME-MG), J. Hydrol., 610, 127948, https://doi.org/10.1016/j.jhydrol.2022.127948, 2022.

Gisolo, D., Bevilacqua, I., Gentile, A., van Ramshorst, J., Patono, D. L., Lovisolo, C., Previati, M., Canone, D., and Ferraris, S.: Evapotranspiration of an abandoned grassland in the Italian Alps: Modeling the impact of shrub encroachment, J. Hydrol., 635, 131223, https://doi.org/10.1016/j.jhydrol.2024.131223, 2024.

Gisolo, D., Gentile, A., Canone, D., and Ferraris, S.: Monitoring Ecohydrological Variables in a Peri-Urban Forest and a Non-glacial High-Elevation Grassland Representing Possible Future Conditions in the Alps, in: Biosystems Engineering Promoting Resilience to Climate Change - AIIA 2024 - Mid-Term Conference, Cham, 83–90, https://doi.org/10.1007/978-3-031-84212-2_11, 2025.

Goldsmith, G. R., Allen, S. T., Braun, S., Engbersen, N., González-Quijano, C. R., Kirchner, J. W., and Siegwolf, R. T. W.: Spatial variation in throughfall, soil, and plant water isotopes in a temperate forest, Ecohydrology, 12, e2059, https://doi.org/10.1002/eco.2059, 2019.

Goldsmith, G. R., Allen, S. T., Braun, S., Siegwolf, R. T. W., and Kirchner, J. W.: Climatic Influences on Summer Use of Winter Precipitation by Trees, Geophys. Res. Lett., 49, e2022GL098323, https://doi.org/10.1029/2022GL098323, 2022.

Harpold, A. A., Kaplan, M. L., Klos, P. Z., Link, T., McNamara, J. P., Rajagopal, S., Schumer, R., and Steele, C. M.: Rain or snow: hydrologic processes, observations, prediction, and research needs, Hydrol. Earth Syst. Sci., 21, 1–22, https://doi.org/10.5194/hess-21-1-2017, 2017.

Harrison, H. N., Hammond, J. C., Kampf, S., and Kiewiet, L.: On the hydrological difference between catchments above and below the intermittent-persistent snow transition, Hydrol. Process., 35, e14411, https://doi.org/10.1002/hyp.14411, 2021.

Hayashi, M.: Alpine Hydrogeology: The Critical Role of Groundwater in Sourcing the Headwaters of the World, Ground Water, 58, 498–510, https://doi.org/10.1111/gwat.12965, 2020.

Hirashima, H., Avanzi, F., and Yamaguchi, S.: Liquid water infiltration into a layered snowpack: evaluation of a 3-D water transport model with laboratory experiments, Hydrol. Earth Syst. Sci., 21, 5503–5515, https://doi.org/10.5194/hess-21-5503-2017, 2017.

Hock, R.: Temperature index melt modelling in mountain areas, J. Hydrol., 282, 104–115, https://doi.org/10.1016/S0022-1694(03)00257-9, 2003.

https://doi.org/10.5194/egusphere-2025-6329
Preprint. Discussion started: 3 February 2026

Hotovy, O., Nedelcev, O., Seibert, J., and Jenicek, M.: Rain-on-snow events in mountainous catchments under climate change, Hydrol. Earth Syst. Sci., 29, 4199–4217, https://doi.org/10.5194/hess-29-4199-2025, 2025.

Jarvis, N.: The MACRO Model (version 3.1). Technical description and sample simulations., 1994.

Kirchner, J. W., Benettin, P., and Meerveld, I. van: Instructive Surprises in the Hydrological Functioning of Landscapes, Annu. Rev. Earth Planet. Sci., 51, 277–299, https://doi.org/10.1146/annurev-earth-071822-100356, 2023.

Koehler, J., Dietz, A. J., Zellner, P., Baumhoer, C. A., Dirscherl, M., Cattani, L., Vlahović, Ž., Alasawedah, M. H., Mayer, K., Haslinger, K., Bertoldi, G., Jacob, A., and Kuenzer, C.: Drought in Northern Italy: Long Earth Observation Time Series Reveal Snow Line Elevation to Be Several Hundred Meters Above Long-Term Average in 2022, Remote Sens., 14, 6091, https://doi.org/10.3390/rs14236091, 2022.

Koeniger, P., Marshall, J. D., Link, T., and Mulch, A.: An inexpensive, fast, and reliable method for vacuum extraction of soil and plant water for stable isotope analyses by mass spectrometry, Rapid Commun. Mass Spectrom., 25, 3041–3048, https://doi.org/10.1002/rcm.5198, 2011.

Landwehr, J. M. and Coplen, T. B.: Line-conditioned excess: A new method for characterizing stable hydrogen and oxygen isotope ratios in hydrologic systems, International Conference on Isotopes in Environmental Studies, Aquatic Forum 2004, Monaco, Vienna, Austria, 132–135, 2006.

Lehning, M., Bartelt, P., Brown, B., Russi, T., Stöckli, U., and Zimmerli, M.: snowpack model calculations for avalanche warning based upon a new network of weather and snow stations, Cold Reg. Sci. Technol., 30, 145–157, https://doi.org/10.1016/S0165-232X(99)00022-1, 1999.

Leroux, N. R. and Pomeroy, J. W.: Modelling capillary hysteresis effects on preferential flow through melting and cold layered snowpacks, Adv. Water Resour., 107, 250–264, https://doi.org/10.1016/j.advwatres.2017.06.024, 2017.

Lundberg, A., Ala-Aho, P., Eklo, O., Klöve, B., Kværner, J., and Stumpp, C.: Snow and frost: implications for spatiotemporal infiltration patterns – a review, Hydrol. Process., 30, 1230–1250, https://doi.org/10.1002/hyp.10703, 2016.

Marchina, C., Zuecco, G., Chiogna, G., Bianchini, G., Carturan, L., Comiti, F., Engel, M., Natali, C., Borga, M., and Penna, D.: Alternative methods to determine the δ2H-δ18O relationship: An application to different water types, J. Hydrol., 587, 124951, https://doi.org/10.1016/j.jhydrol.2020.124951, 2020.

Mastrotheodoros, T., Pappas, C., Molnar, P., Burlando, P., Manoli, G., Parajka, J., Rigon, R., Szeles, B., Bottazzi, M., Hadjidoukas, P., and Fatichi, S.: More green and less blue water in the Alps during warmer summers, Nat. Clim. Change, 10, 155–161, https://doi.org/10.1038/s41558-019-0676-5, 2020.

McDonnell, J. J.: The two water worlds hypothesis: ecohydrological separation of water between streams and trees?, WIREs Water, 1, 323–329, https://doi.org/10.1002/wat2.1027, 2014.

McDonnell, J. J.: Beyond the water balance, Nat. Geosci., 10, 396, https://doi.org/10.1038/ngeo2964, 2017.

McDonnell, J. J., Spence, C., Karran, D. J., van Meerveld, H. J. (Ilja), and Harman, C. J.: Fill-and-Spill: A Process Description of Runoff Generation at the Scale of the Beholder, Water Resour. Res., 57, e2020WR027514, https://doi.org/10.1029/2020WR027514, 2021.

Michelon, A., Ceperley, N., Beria, H., Larsen, J., Vennemann, T., and Schaefli, B.: Hydrodynamics of a high Alpine catchment characterized by four natural tracers, Hydrol. Earth Syst. Sci., 27, 1403–1430, https://doi.org/10.5194/hess-27-1403-2023, 2023.

Millar, C., Janzen, K., Nehemy, M. F., Koehler, G., Hervé-Fernández, P., Wang, H., Orlowski, N., Barbeta, A., and McDonnell, J. J.: On the urgent need for standardization in isotope-based ecohydrological investigations, Hydrol. Process., 36, e14698, https://doi.org/10.1002/hyp.14698, 2022.

Millington, R. J. and Quirk, J. P.: Permeability of porous solids, Trans. Faraday Soc., 57, 1200–1207, https://doi.org/10.1039/TF9615701200, 1961.

Mohammed, A. A., Pavlovskii, I., Cey, E. E., and Hayashi, M.: Effects of preferential flow on snowmelt partitioning and groundwater recharge in frozen soils, Hydrol. Earth Syst. Sci., 23, 5017–5031, https://doi.org/10.5194/hess-23-5017-2019, 2019.

Mualem, Y.: A new model for predicting the hydraulic conductivity of unsaturated porous media, Water Resour. Res., 12, 513–522, https://doi.org/10.1029/WR012i003p00513, 1976.

Myers, D. T., Ficklin, D. L., and Robeson, S. M.: Hydrologic implications of projected changes in rain-on-snow melt for Great Lakes Basin watersheds, Hydrol. Earth Syst. Sci., 27, 1755–1770, https://doi.org/10.5194/hess-27-1755-2023, 2023.

Nasta, P., Todini-Zicavo ,Diego, Zuecco ,Giulia, Marchina ,Chiara, Penna ,Daniele, McDonnell ,Jeffrey J., Amin ,Anam, Allocca ,Carolina, Marzaioli ,Fabio, Stellato ,Luisa, Borga ,Marco, and and Romano, N.: Quantifying irrigation uptake in olive trees: a proof-of-concept approach combining isotope tracing and Hydrus-1D, Hydrol. Sci. J., 68, 1479–1486, https://doi.org/10.1080/02626667.2023.2218552, 2023.

Nehemy, M. F., Maillet, J., Perron, N., Pappas, C., Sonnentag, O., Baltzer, J. L., Laroque, C. P., and McDonnell, J. J.: Snowmelt Water Use at Transpiration Onset: Phenology, Isotope Tracing, and Tree Water Transit Time, Water Resour. Res., 58, e2022WR032344, https://doi.org/10.1029/2022WR032344, 2022.

Nimmo, J. R.: Porosity and Pore Size Distribution☆, in: Reference Module in Earth Systems and Environmental Sciences, Elsevier, https://doi.org/10.1016/B978-0-12-409548-9.05265-9, 2013.

Orlowski, N., Breuer, L., and McDonnell, J. J.: Critical issues with cryogenic extraction of soil water for stable isotope analysis, Ecohydrology, 9, 1–5, https://doi.org/10.1002/eco.1722, 2016a.

Orlowski, N., Pratt, D. L., and McDonnell, J. J.: Intercomparison of soil pore water extraction methods for stable isotope analysis, Hydrol. Process., 30, 3434–3449, https://doi.org/10.1002/hyp.10870, 2016b.

Orlowski, N., Breuer, L., Angeli, N., Boeckx, P., Brumbt, C., Cook, C. S., Dubbert, M., Dyckmans, J., Gallagher, B., Gralher, B., Herbstritt, B., Hervé-Fernández, P., Hissler, C., Koeniger, P., Legout, A., Macdonald, C. J., Oyarzún, C., Redelstein, R., Seidler, C., Siegwolf, R., Stumpp, C., Thomsen, S., Weiler, M., Werner, C., and McDonnell, J. J.: Inter-laboratory comparison of cryogenic water extraction systems for stable isotope analysis of soil water, Hydrol. Earth Syst. Sci., 22, 3619–3637, https://doi.org/10.5194/hess-22-3619-2018, 2018.

Orlowski, N., Rinderer, M., Dubbert, M., Ceperley, N., Hrachowitz, M., Gessler, A., Rothfuss, Y., Sprenger, M., Heidbüchel, I., Kübert, A., Beyer, M., Zuecco, G., and McCarter, C.: Challenges in studying water fluxes within the soil-plant-atmosphere continuum: A tracer-based perspective on pathways to progress, Sci. Total Environ., 881, 163510, https://doi.org/10.1016/j.scitotenv.2023.163510, 2023.

https://doi.org/10.5194/egusphere-2025-6329
Preprint. Discussion started: 3 February 2026

Painter, K. J., Gentile, A., and Ferraris, S.: A stochastic cellular automaton model to describe the evolution of the snow-covered area across a high-elevation mountain catchment, Sci. Total Environ., 857, 159195, https://doi.org/10.1016/j.scitotenv.2022.159195, 2023.

Pavlovskii, I., Hayashi, M., and Lennon, M. R.: Transformation of snow isotopic signature along groundwater recharge pathways in the Canadian Prairies, J. Hydrol., 563, 1147–1160, https://doi.org/10.1016/j.jhydrol.2017.09.053, 2018.

Penna, D., Oliviero, O., Assendelft, R., Zuecco, G., Meerveld, I. (H. J.) van, Anfodillo, T., Carraro, V., Borga, M., and Fontana, G. D.: Tracing the Water Sources of Trees and Streams: Isotopic Analysis in a Small Pre-Alpine Catchment, Procedia Environ. Sci., 19, 106–112, https://doi.org/10.1016/j.proenv.2013.06.012, 2013.

Penna, D., Hopp, L., Scandellari, F., Allen, S. T., Benettin, P., Beyer, M., Geris, J., Klaus, J., Marshall, J. D., Schwendenmann, L., Volkmann, T. H. M., von Freyberg, J., Amin, A., Ceperley, N., Engel, M., Frentress, J., Giambastiani, Y., McDonnell, J. J., Zuecco, G., Llorens, P., Siegwolf, R. T. W., Dawson, T. E., and Kirchner, J. W.: Ideas and perspectives: Tracing terrestrial ecosystem water fluxes using hydrogen and oxygen stable isotopes – challenges and opportunities from an interdisciplinary perspective, Biogeosciences, 15, 6399–6415, https://doi.org/10.5194/bg-15-6399-2018, 2018.

Radolinski, J., Pangle, L., Klaus, J., and Stewart, R. D.: Testing the 'two water worlds' hypothesis under variable preferential flow conditions, Hydrol. Process., 35, e14252, https://doi.org/10.1002/hyp.14252, 2021.

Ravazzani, G., Corbari, C., Morella, S., Gianoli, P., and Mancini, M.: Modified Hargreaves-Samani Equation for the Assessment of Reference Evapotranspiration in Alpine River Basins, J. Irrig. Drain. Eng., 138, 592–599, https://doi.org/10.1061/(ASCE)IR.1943-4774.0000453, 2012.

Renée Brooks, J., Barnard, H. R., Coulombe, R., and McDonnell, J. J.: Ecohydrologic separation of water between trees and streams in a Mediterranean climate, Nat. Geosci., 3, 100–104, https://doi.org/10.1038/ngeo722, 2010.

Rigon, R., Bertoldi, G., and Over, T. M.: GEOtop: A Distributed Hydrological Model with Coupled Water and Energy Budgets, J. Hydrometeorol., 7, 371–388, https://doi.org/10.1175/JHM497.1, 2006.

Ritchie, J. T.: Model for predicting evaporation from a row crop with incomplete cover, Water Resour. Res., 8, 1204–1213, https://doi.org/10.1029/WR008i005p01204, 1972.

Scandellari, F. and Penna, D.: Gli isotopi stabili nell'acqua fra suolo, pianta e atmosfera, Italus Hortus, 51–67, https://doi.org/10.26353/j.itahort/2017.2.5167, 2018.

Schaefli, B., Nicótina, L., Imfeld, C., Da Ronco, P., Bertuzzo, E., and Rinaldo, A.: SEHR-ECHO v1.0: a Spatially Explicit Hydrologic Response model for ecohydrologic applications, Geosci. Model Dev., 7, 2733–2746, https://doi.org/10.5194/gmd-7-2733-2014, 2014.

Šimůnek, J., Šejna, M., Saito, H., Sakai, M., and van Genuchten, M. Th.: The HYDRUS-1D Software Package for Simulating the One-Dimensional Movement of Water, Heat, and Multiple Solutes in Variably-Saturated Media, Department of Environmental Sciences, University of California Riverside, Riverside, California, 2018.

Sprenger, M. and Allen, S. T.: What Ecohydrologic Separation Is and Where We Can Go With It, Water Resour. Res., 56, e2020WR027238, https://doi.org/10.1029/2020WR027238, 2020.

Sprenger, M., Leistert, H., Gimbel, K., and Weiler, M.: Illuminating hydrological processes at the soil-vegetation-atmosphere interface with water stable isotopes, Rev. Geophys., 54, 674–704, https://doi.org/10.1002/2015RG000515, 2016.

https://doi.org/10.5194/egusphere-2025-6329
Preprint. Discussion started: 3 February 2026

880 Strasser, U., Warscher, M., Rottler, E., and Hanzer, F.: openAMUNDSEN v 0.8.3: an open source snow-hydrological model for mountain regions, EGUsphere, 1–25, https://doi.org/10.5194/egusphere-2024-193, 2024.

Stumpp, C., Stichler, W., Kandolf, M., and Šimůnek, J.: Effects of Land Cover and Fertilization Method on Water Flow and Solute Transport in Five Lysimeters: A Long-Term Study Using Stable Water Isotopes, Vadose Zone J., 11, https://doi.org/10.2136/vzj2011.0075, 2012.

885 van Tiel, M., Aubry-Wake, C., Somers, L., Andermann, C., Avanzi, F., Baraer, M., Chiogna, G., Daigre, C., Das, S., Drenkhan, F., Farinotti, D., Fyffe, C. L., de Graaf, I., Hanus, S., Immerzeel, W., Koch, F., McKenzie, J. M., Müller, T., Popp, A. L., Saidaliyeva, Z., Schaefli, B., Schilling, O. S., Teagai, K., Thornton, J. M., and Yapiyev, V.: Cryosphere–groundwater connectivity is a missing link in the mountain water cycle, Nat. Water, 2, 624–637, https://doi.org/10.1038/s44221-024-00277-8, 2024.

890 Van Mullem, J. A., Garen, D., and Woodward, D. E.: Part 630 Hydrology National Engineering Handbook - Chapter 11, 2004.

Vionnet, V., Brun, E., Morin, S., Boone, A., Faroux, S., Le Moigne, P., Martin, E., and Willemet, J.-M.: The detailed snowpack scheme Crocus and its implementation in SURFEX v7.2, Geosci. Model Dev., 5, 773–791, https://doi.org/10.5194/gmd-5-773-2012, 2012.

895 White, J. W. C.: Stable Hydrogen Isotope Ratios in Plants: A Review of Current Theory and Some Potential Applications, in: Stable Isotopes in Ecological Research, New York, NY, 142–162, https://doi.org/10.1007/978-1-4612-3498-2_10, 1989.

Winograd, I. J., Riggs, A. C., and Coplen, T. B.: The relative contributions of summer and cool-season precipitation to groundwater recharge, Spring Mountains, Nevada, USA, Hydrogeol. J., 6, 77–93, https://doi.org/10.1007/s100400050135, 1998.

900 Zhou, S., Nakawo, M., Hashimoto, S., and Sakai, A.: The effect of refreezing on the isotopic composition of melting snowpack, Hydrol. Process., 22, 873–882, https://doi.org/10.1002/hyp.6662, 2008.

Zhou, T., Šimůnek, J., and Braud, I.: Adapting HYDRUS-1D to simulate the transport of soil water isotopes with evaporation fractionation, Environ. Model. Softw., 143, 105118, https://doi.org/10.1016/j.envsoft.2021.105118, 2021.

Zuecco, G., Amin, A., Frentress, J., Engel, M., Marchina, C., Anfodillo, T., Borga, M., Carraro, V., Scandellari, F., Tagliavini,
905 M., Zanotelli, D., Comiti, F., and Penna, D.: A comparative study of plant water extraction methods for isotopic analyses: Scholander-type pressure chamber vs. cryogenic vacuum distillation, Hydrol. Earth Syst. Sci., 26, 3673–3689, https://doi.org/10.5194/hess-26-3673-2022, 2022.

Zuecco, G., Gentile, A., Nasta, P., Brighenti, S., Allocca, C., Bertoldi, G., Canone, D., Comiti, F., Fabiani, G., Ferraris, S., Villahermosa, F. M. di, Marchina, C., Marzaioli, F., Penna, D., Previati, M., Romano, N., Stellato, L., Todini-Zicavo, D., and
910 Borga, M.: Investigating the seasonal origin of soil and xylem water in Italian mountain catchments, Copernicus Meetings, https://doi.org/10.5194/egusphere-egu24-12737, 2024.

Zuecco, G., Todini-Zicavo, D., Marchina, C., Brighenti, S., Penna, D., and Borga, M.: Trees use predominantly summer water in a pre-Alpine catchment, J. Hydrol., 664, 134430, https://doi.org/10.1016/j.jhydrol.2025.134430, 2026.